NUMERICAL AND EXPERIMENTAL STUDY OF MULTICHARGED ION BEAM EXTRACTION FROM ELECTRON CYCLOTRON RESONANCE ION SOURCE

Antonio Méndez Giono

Under the supervision of Thomas Thuillier[1] & Tiberiu Minea[2]

[1]Université Grenoble-Alpes, CNRS-IN2P3, Grenoble Institute of Engineering (INP), LPSC, 38000 Grenoble, France
[2]Université Paris-Saclay, CNRS-IN2P3, LPGP, 91405 Orsay, Île de France, France

Séminaire doctorant, 29 March 2021

-Presentation outline-

- Introduction
  - Project overview
  - Electron cyclotron resonance (ECR) ion sources
- Guiding centre particle pusher
  - The model
  - Results
- Self-consistent Monte-Carlo ECR plasma simulation (in development)
  - Multipole magnetic field model
  - Overview
  - Collision handling
- Beam transport simulation
  - The low energy beam transport (LEBT) line
  - Magnet and extraction array modelling (RADIA & OPERA & POISSON SUPERFISH)
- Project prospects and conclusions

INTRODUCTION

-Introduction- The project

- This project aims to develop a simulation framework to aid in the design and development of electron cyclotron resonance (ECR) ion sources.

- Develop and/or adapt 3 simulation codes able to reproduce the experimental beam emittance for ECR ion sources
  - A self-consistent Monte-Carlo ECR ion source plasma simulation
  - A Particle-In-Cell ion beam extraction simulation (ONIX-LPGP)
  - Beam transport simulation

- Validate the simulation results through experimental emittance measurements
  - A Low Energy Beam Transport (LEBT) incorporating the PHOENIX V2 ECR ion source (developed at LPSC)
  - Allison type emittance scanners as to measure the extracted beam's 4D transversal emittance.

-Introduction-
ECR ion sources

- Electron confinement is achieved via magnetic mirror bouncing in a **Minimum-B** configuration.
- Microwaves at the cyclotron frequency heat up the ionising electrons at the **ECR surface**. $\omega_{RF} = \omega_c = eB/m_e$
- Ions are created in a magnetically confined plasma by electron impact ionisation from a population on ”warm” electrons (1-10keV).
- The ion beam is then extracted by an electrostatic potential.

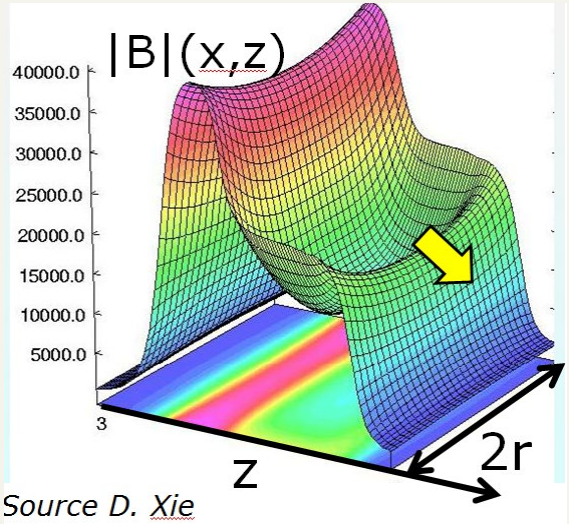

Min-B configuration

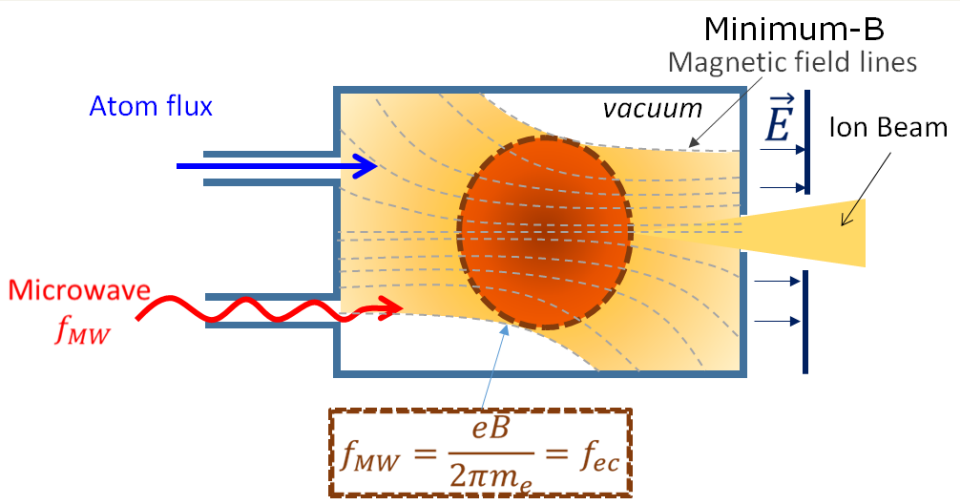

ECR ion source schema

-Introduction-
ECR electron energy distributions

- The interactions leading to the electron energy distribution are very complex and its exact form is not well known to this date.
  - A population of cold electrons (1-100 eV): Very weakly confined and not ionising. Blue
  - A population of warm electrons (1-10 keV): Well confined and responsible for ionisation. Red
  - A population of hot electrons (10-500 keV): Do not interact by collision, thought to be important for the confinement of ions. Orange

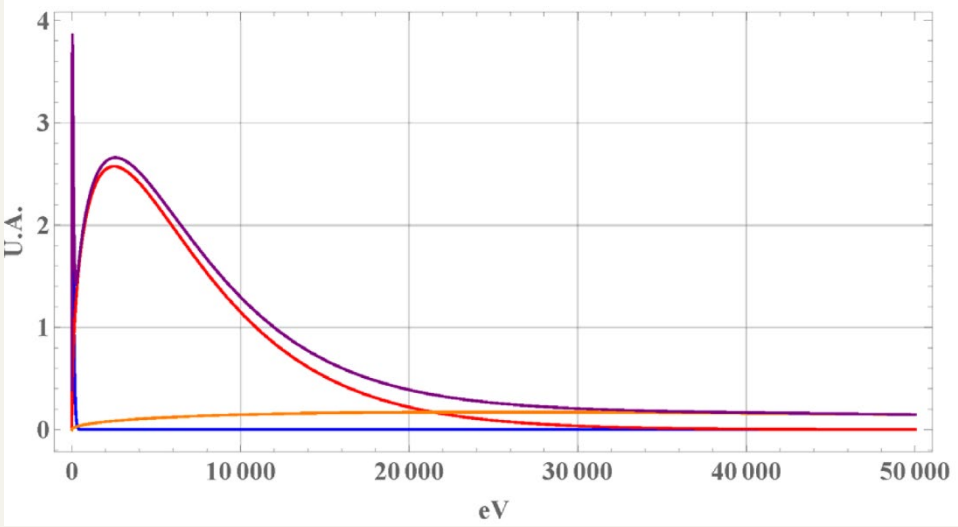

Different electron populations in an ECR ion source, purple is the aggregate. (Thuillier)

-Introduction-
ECR - Species confinement

Electron confinement

- Magnetically confined
- Given a small gradient condition, $\rho_L \ll \frac{B}{|\nabla B|}$, the magnetic moment is an adiabatic invariant.

$$\mu = mv_\perp^2/2B$$

$$T = \frac{1}{2}mv_\parallel^2 + \mu B$$

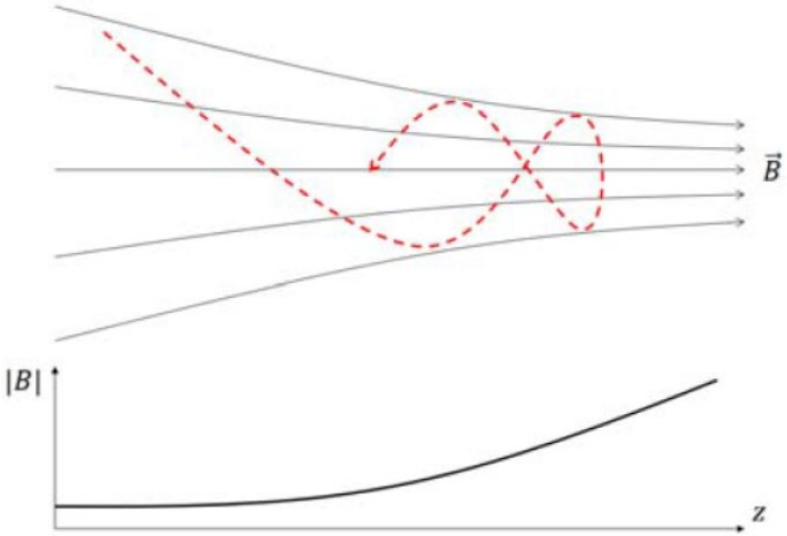

Ion confinement

- For ions, magnetic confinement with coulomb scattering gives a confinement time much smaller than what is observed (1-1000 ms).
- It is thought that a high ”hot” electron density at the centre creates a potential dip which electrostatically confines the ions in the ECR region (volume contained in the ECR surface).
- This potential dip has yet to be reproduced in simulation.

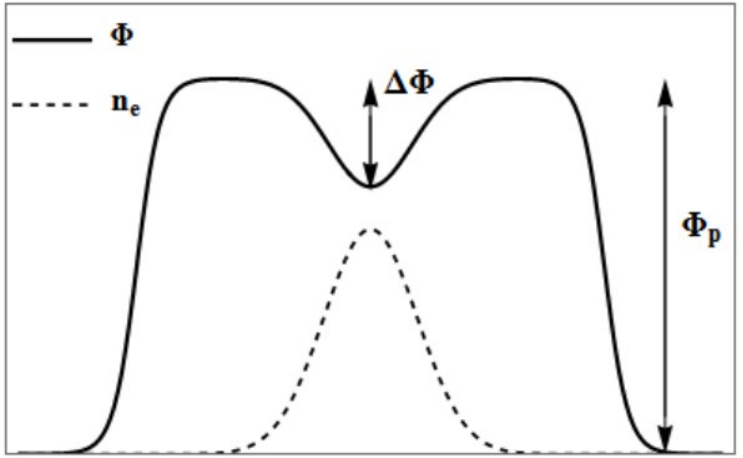

-Introduction-
Simulation objective

Reproduce the emittance of an extracted ion beam from an ECR ion source

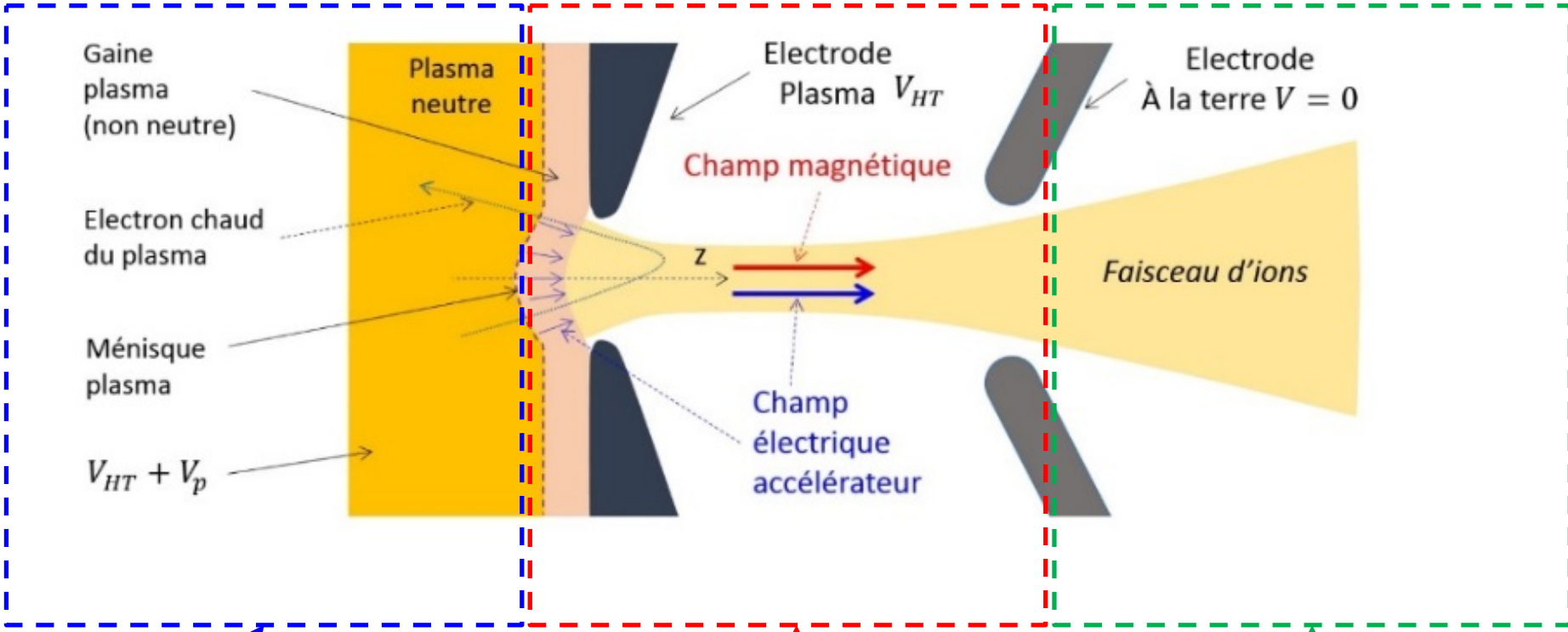

Self-consistent 3DMonte Carlo

inputs

ONIX PIC 3D

outputs

Beam transport code

-Introduction-
Phoenix V2 ECRIS

- Compact ECRIS commissioned for the SPIRAL2 accelerator.
- 0.6L plasma chamber volume (L204mm , Ø63mm)
- Operation frequency of 18GHz

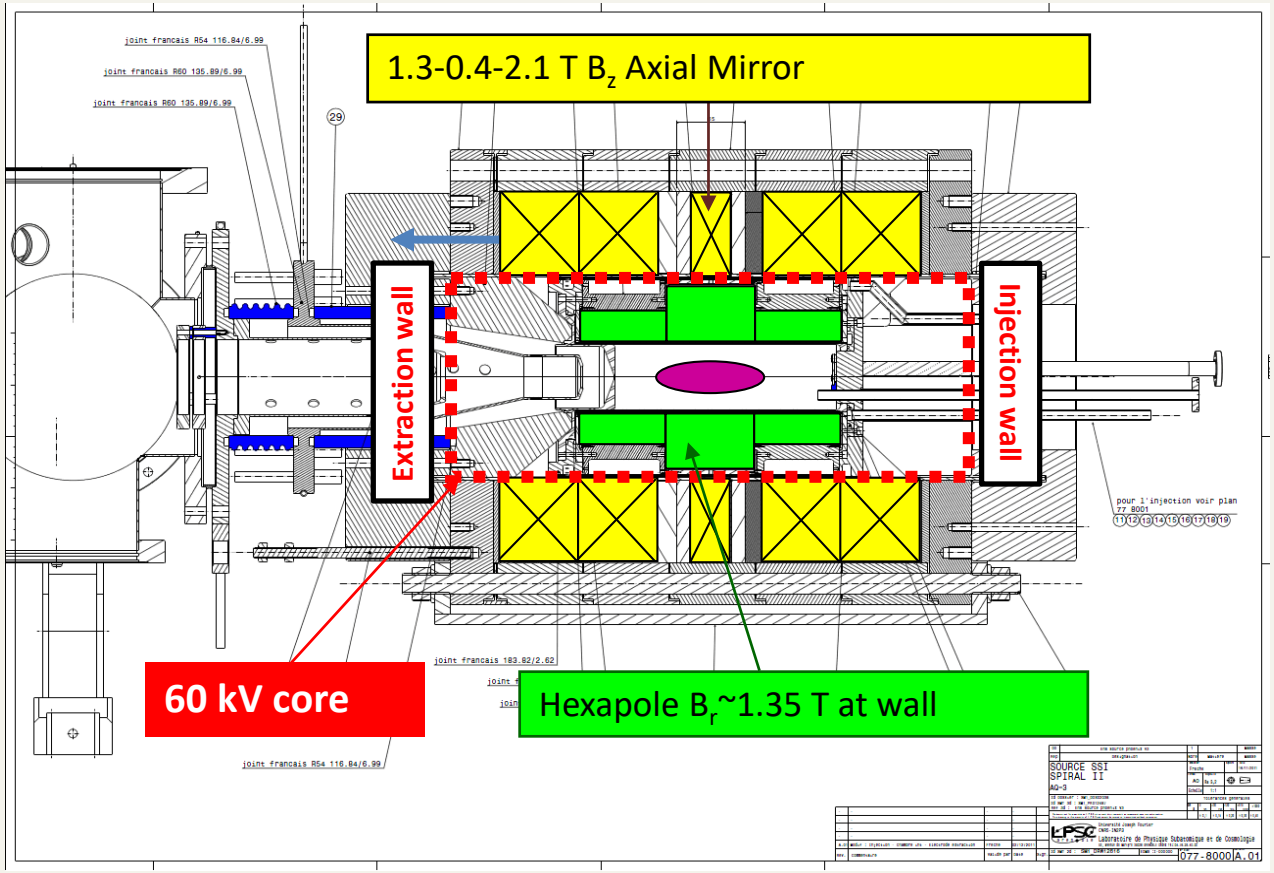

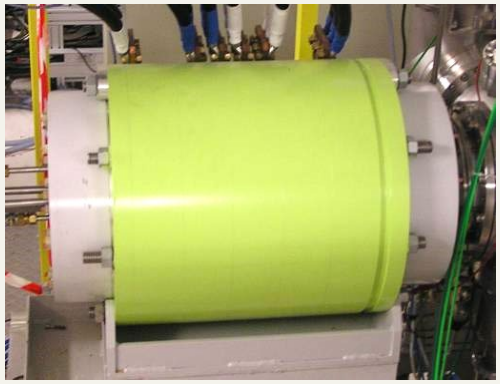

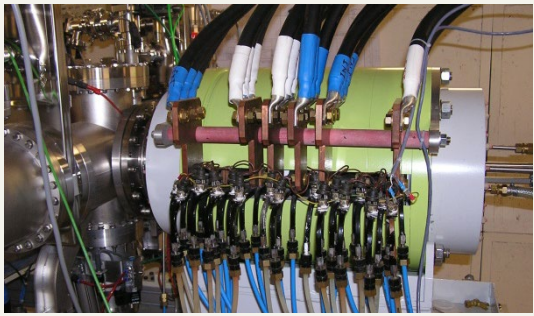

GUIDING CENTRE (GC) PARTICLE PUSHER

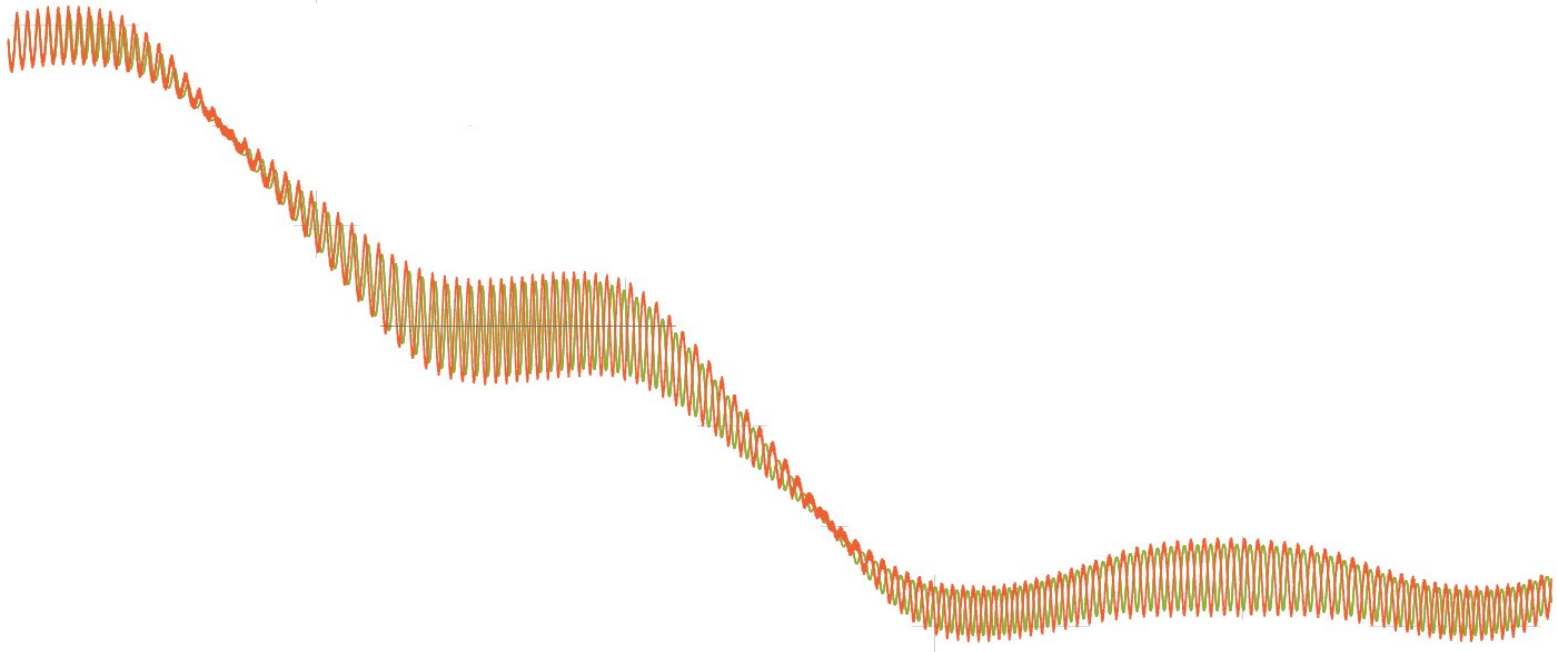

-GC particle pusher-

- Objective: Investigation of the validity and stability of the Guiding Centre (GC) algorithm to speed up particle propagation in magnetised plasma simulation.

- Methodology:
  - Implementation of two, otherwise identical, algorithms in c to simulate electron trajectories by Boris and the GC approximation.
  - Consistency check and computation time measurement of trajectories for equivalent initial conditions with different time-steps (dt).
  - Identify a range of validity for the propagation time-step (dt).

- Work in this section was given as a talk in the 24th International Workshop on ECR Ion Sources (ECRIS'20) and published in the proceedings.

-GC particle pusher- The model

- Condition:
  - The magnetic dipole moment (μ) is an adiabatic invariant if the motion along the plasma chamber is slow compared to the cyclotron motion .
  - Equivalently, the Larmor radius should be much smaller than the length scale of ∇B.

$$\rho_L \ll \frac{B}{|\nabla B|}$$

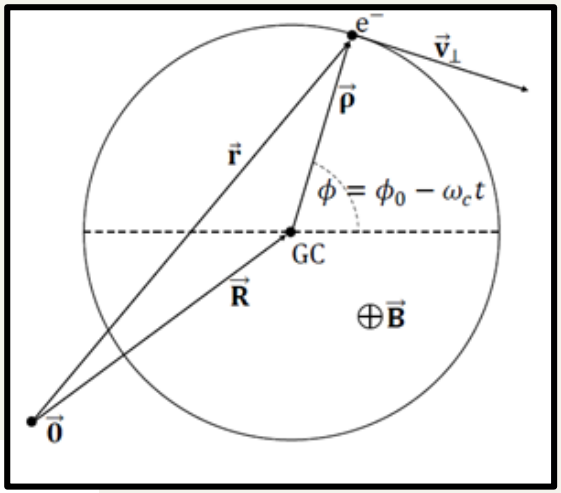

$$\frac{d\mathbf{R}}{dt} = v_{\parallel}\hat{\mathbf{b}} - \overbrace{\frac{\hat{\mathbf{b}}\times\mathbf{E}}{B}}^{\text{crossed fields}} + \frac{\hat{\mathbf{b}}}{B\left(1-\frac{E_\perp^2}{B^2}\right)} \times \left\{ \frac{m\gamma}{q} \overbrace{\left(v_{\parallel}^2(\hat{\mathbf{b}}\cdot\nabla)\hat{\mathbf{b}} + v_{\parallel}(\mathbf{u}\cdot\nabla)\hat{\mathbf{b}} + v_{\parallel}(\hat{\mathbf{b}}\cdot\nabla)\mathbf{u} + (\mathbf{u}\cdot\nabla)\mathbf{u}\right)}^{\text{curvature and polarisation drift}} + \right.$$

$$\underbrace{\frac{\mu}{\gamma q}\nabla\left[B\left(1-\frac{E_\perp^2}{B^2}\right)^{1/2}\right]}_{\text{grad B drift}} + \underbrace{\frac{v_{\parallel}E_{\parallel}}{c^2}\mathbf{u}}_{\text{relativistic}} \left.\right\} \quad \text{with} \quad \mathbf{u} = \mathbf{E}\times\frac{\hat{\mathbf{b}}}{B} \quad \text{and} \quad \underbrace{\frac{d(m\gamma^{*2}v_\perp^{*2}/(2B^*))}{dt} = \frac{d\mu^*}{dt} = 0}_{\mu \text{ invariance } (*=\text{frame of reference at } \mathbf{u})}$$

$$\frac{d(\gamma v_{\parallel})}{dt} = \underbrace{\gamma\mathbf{u}\cdot(v_{\parallel}(\hat{\mathbf{b}}\cdot\nabla)\hat{\mathbf{b}} + (\mathbf{u}\cdot\nabla)\hat{\mathbf{b}})}_{\text{direction change: } \mathbf{u}, v_{\parallel} \text{ exchange}} + \underbrace{\frac{q}{m}E_{\parallel}}_{\mathbf{E}\text{ acc.}} - \underbrace{\frac{\mu}{\gamma m}\hat{\mathbf{b}}\cdot\nabla\left[B\left(1-\frac{E_\perp^2}{B^2}\right)^{1/2}\right]}_{\text{grad. B mirror force}}$$

- Coupled equations solved numerically by RK4 for trajectory integration

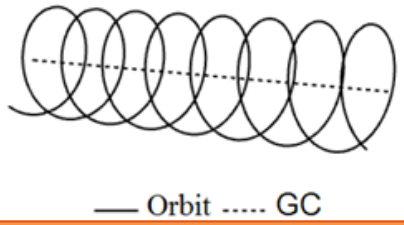

P. O. Vandervoort, "The relativistic motion of a charged particle in an inhomogeneous electromagnetic field, "Annals of Physics, vol. 10, no. 3, pp. 401– 453, 1960.

GC particle pusher
FFA ECR orbit analysis

- GC algorithm ~20 times more computationally expensive per step.
  - ~10^2 times larger timestep rends it faster.
- The GC trajectories are stable up to a 100ps time-step, broken at a 1000ps.
- GC algorithm is able to reduce the CPU time by a factor of 10 wrt Boris.

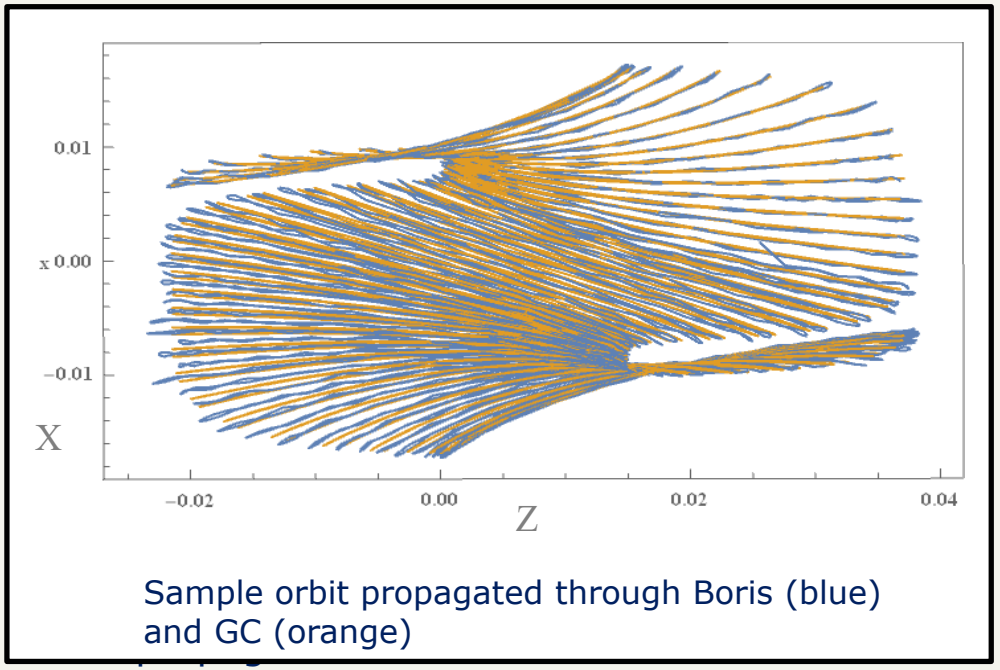

Sample orbit propagated through Boris (blue) and GC (orange)

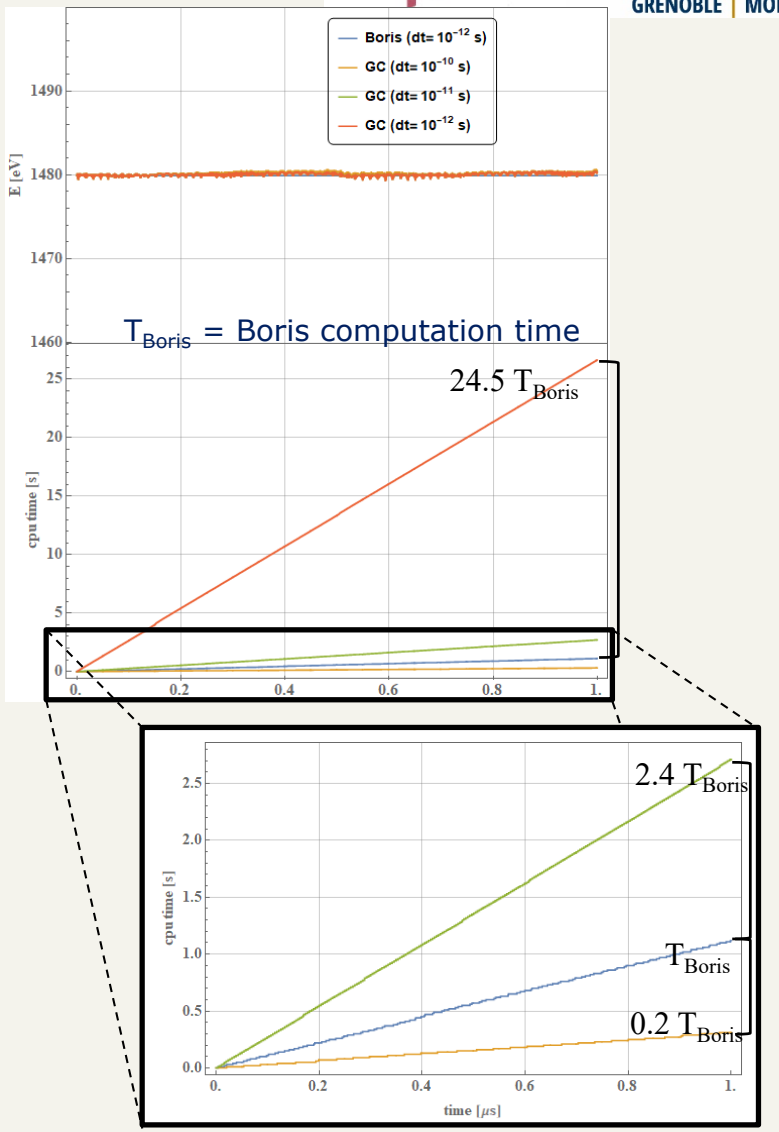

Energy and CPU time for a FFA electron trajectory

-GC particle pusher- ECR confinement

- Good agreement for the confined electron distribution with both propagation methods
  - Sample size 1000, largest valid dt (10^{-10}s for GC and 10^{-12}s for Boris)

Boris propagated e-

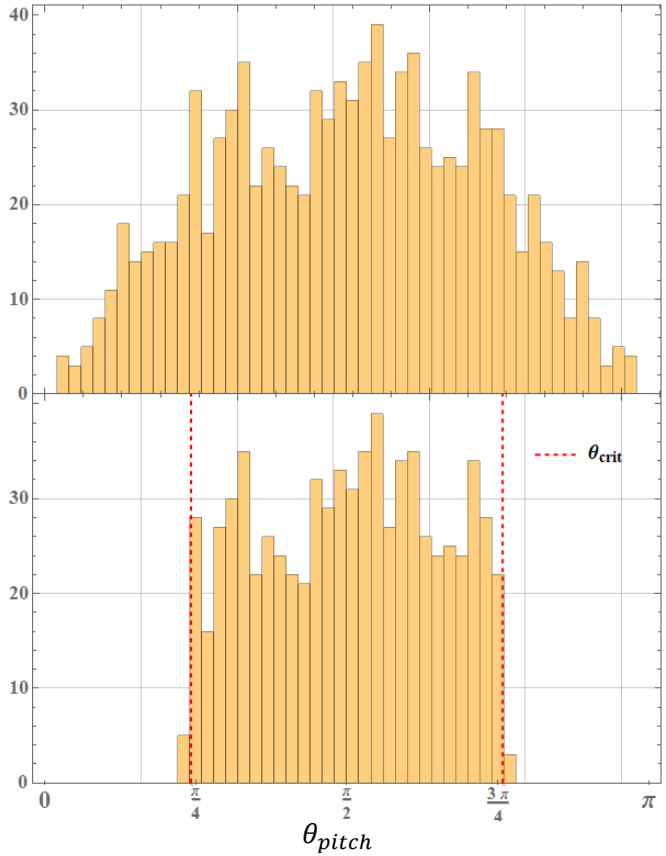

GC propagated e-

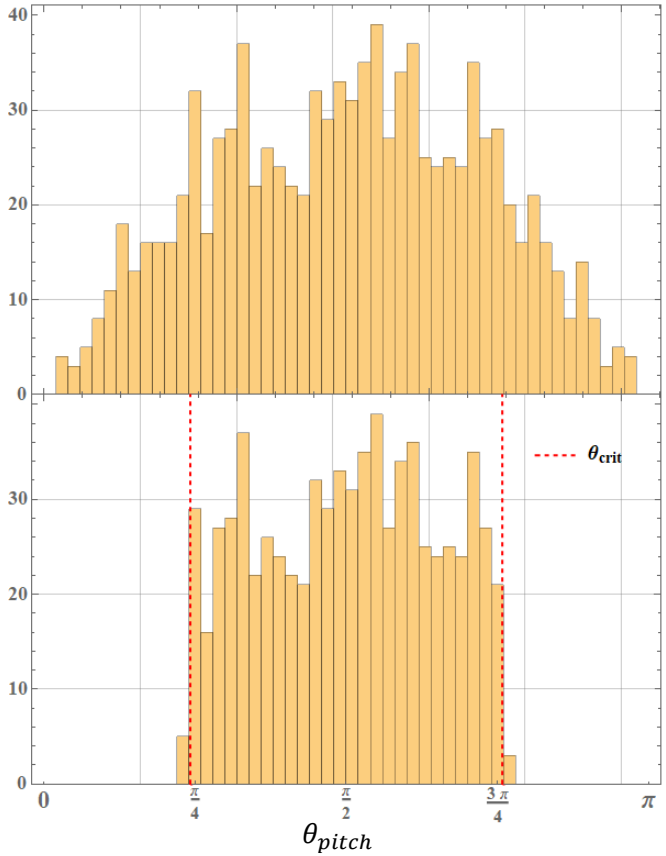

$$\tan(\theta_{pitch}) = \frac{v_\perp}{v_\parallel}$$

$$\frac{1}{\mathcal{R}} = \frac{B_0}{B_{max}}$$

$$\sin(\theta_{crit}) = \frac{1}{\sqrt{\mathcal{R}}}$$

MONTE-CARLO ECR PLASMA SIMULATION

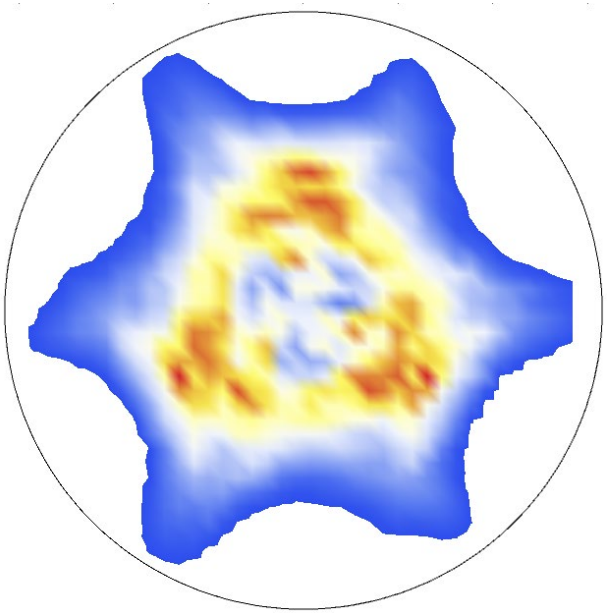

-MC ECR plasma simulation- Multipole magnetic field model

- An analytical first order model for a permanent magnet multipole was derived, including the axial fringe field, with one free parameter (λ).
- Setting the multipole's cavity radius, length, and on axis field, one can get the multipole's magnetic field throughout and just outside the cavity (fringe field).
- For use in simulation applications when fast analytical B computation is required.

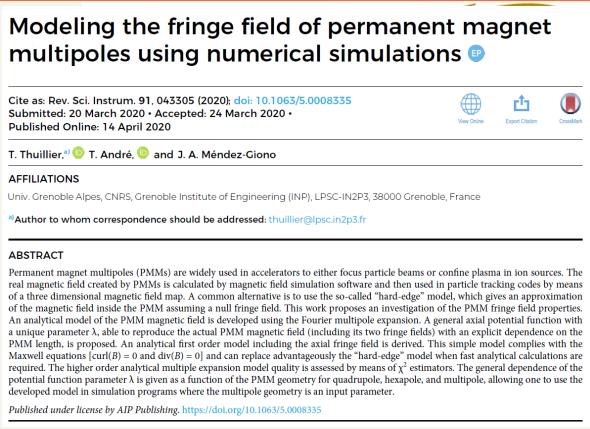

Modeling the fringe field of permanent magnet multipoles using numerical simulations

Cite as: Rev. Sci. Instrum. 91, 043305 (2020); doi: 10.1063/5.0008335
Submitted: 20 March 2020 • Accepted: 24 March 2020 •
Published Online: 14 April 2020

T. Thuillier,[a] T. André, and J. A. Méndez-Giono

AFFILIATIONS

Univ. Grenoble Alpes, CNRS, Grenoble Institute of Engineering (INP), LPSC-IN2P3, 38000 Grenoble, France

[a] Author to whom correspondence should be addressed: thuillier@lpsc.in2p3.fr

ABSTRACT

Permanent magnet multipoles (PMMs) are widely used in accelerators to either focus particle beams or confine plasma in ion sources. The real magnetic field created by PMMs is calculated by magnetic field simulation software and then used in particle tracking codes by means of a three dimensional magnetic field map. A common alternative is to use the so-called "hard-edge" model, which gives an approximation of the magnetic field inside the PMM assuming a null fringe field. This work proposes an investigation of the PMM fringe field properties. An analytical model of the PMM magnetic field is developed using the Fourier multipole expansion. A general axial potential function with a unique parameter λ, able to reproduce the actual PMM magnetic field (including its two fringe fields) with an explicit dependence on the PMM length, is proposed. An analytical first order model including the axial fringe field is derived. This simple model complies with the Maxwell equations [curl(B) = 0 and div(B) = 0] and can replace advantageously the "hard-edge" model when fast analytical calculations are required. The higher order analytical multiple expansion model quality is assessed by means of χ^2 estimators. The general dependence of the potential function parameter λ is given as a function of the PMM geometry for quadrupole, hexapole, and multipole, allowing one to use the developed model in simulation programs where the multipole geometry is an input parameter.

Published in Rev. Sci. Instrum. In collaboration with Thomas Thuillier and Thomas André (LPSC)

$$B_r = B_0\left(\frac{r}{R_0}\right)^{m-1} f_{\lambda,L}(z)\cos(m\theta),$$

$$B_\theta = -B_0\left(\frac{r}{R_0}\right)^{m-1} f_{\lambda,L}(z)\sin(m\theta),$$

$$B_z = \frac{B_0 R_0}{m}\left(\frac{r}{R_0}\right)^{m} f'_{\lambda,L}(z)\cos(m\theta),$$

$$f_{\lambda,L}(z) = \frac{1}{\left(1+e^{\lambda\left(z-\frac{L}{2}\right)}\right)\left(1+e^{-\lambda\left(z+\frac{L}{2}\right)}\right)}$$

$$f'_{\lambda,L}(z) = -\lambda\left(e^{\lambda\left(z-\frac{L}{2}\right)} - e^{-\lambda\left(z+\frac{L}{2}\right)}\right) f^2_{\lambda,L}(z)$$

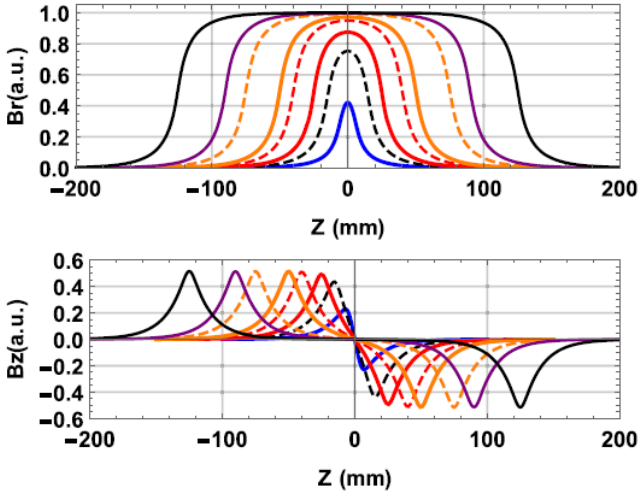

FIG. 3. Evolution of the radial (top) and axial (bottom) magnetic field profiles along z as a function of *L* for a PMM hexapole. The radial intensity is normalized to 1. The different plots correspondto L=10 (blue), 30, 80, 100, 150,180,200 mm (black).

-MC ECR plasma simulation-

- Objective: Develop a self consistent Monte-Carlo simulation of the plasma for the PHOENIX V2 ERC ion source capable of reproducing the current ion charge and energy distributions around the extraction aperture.
- Methodology:
  - Implementation of a code for propagating electrons and ions of a Helium plasma inside the source's plasma chamber.
  - Implement a meshing system for keeping the charge, energy and spatial distributions of the species between iterations.
  - Handling of coulomb collisions between the species (Takizuka-Abe (TA) method).
  - Handling of inelastic collisions relevant to the charge state, energy and spatial distributions of the species (null-collision method).
  - Solve Maxwell equations with the obtained distributions and incorporate the electromagnetic field to the propagation.
  - Implement heating through simulating the propagation of injected microwaves to the source.

-MC ECR plasma simulation- Code overview

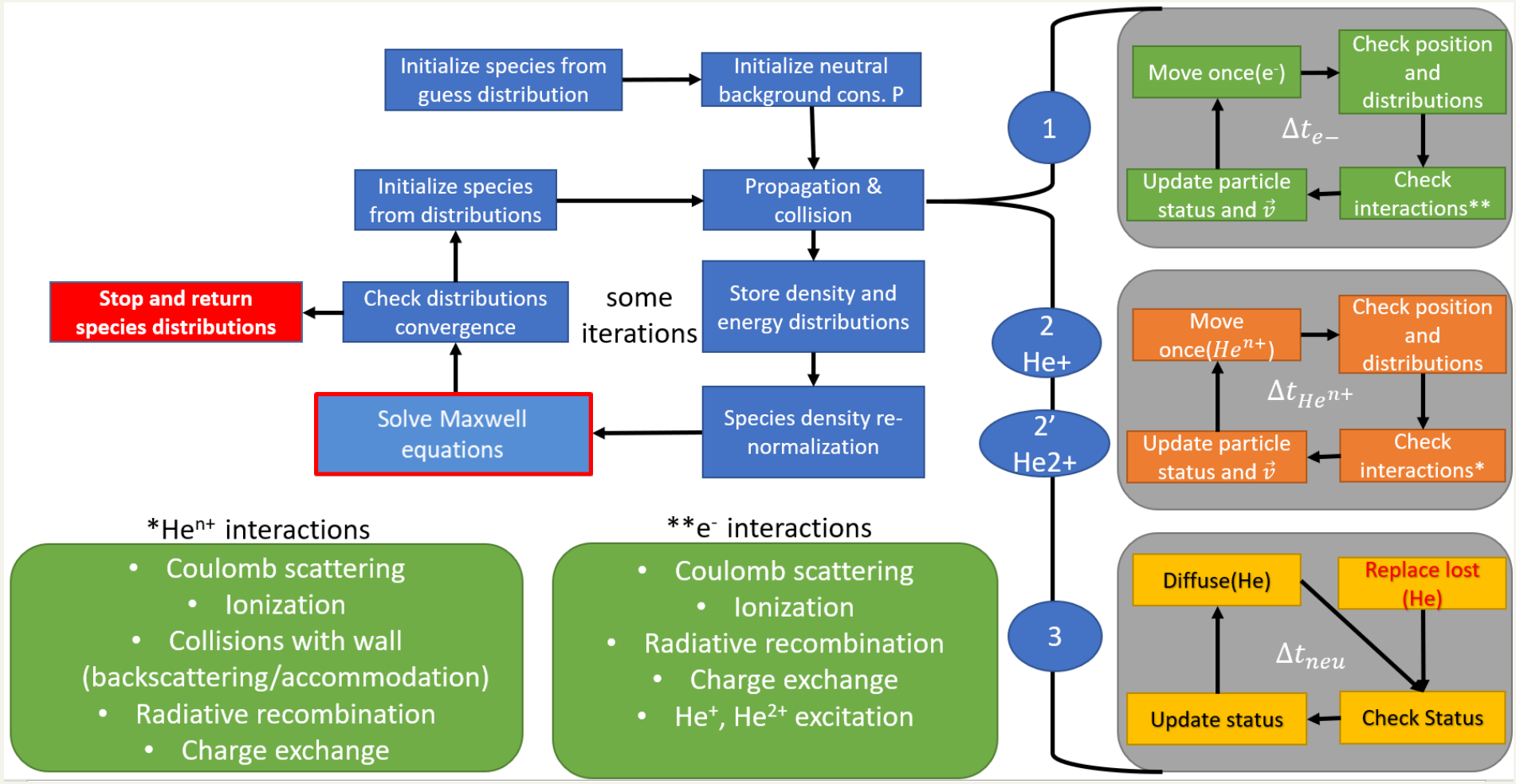

$$\Delta t_{e-} < \Delta t_{He^{n+}} < \Delta t_{neu}$$

-MC ECR plasma simulation- Density and energy comp.

- In each cell of the mesh are saved at each propagation step:
  - Particle count ($N_{part\ cell}$)
  - Parallel ($v_{\parallel}$) and perpendicular ($v_{\perp}$) speed distributions (with respect to the magnetic field). This are used to generate random collision partners during propagation.
- After a particles' propagation loop finalizes:
  - The count is renormalized to density at first as: $\mathrm{n_{cell}}\ [\mathrm{m^{-3}}] = n_0 \left(\frac{V_{pc}}{V_{cell}}\right)\left(\frac{N_{part\ cell}}{N_{part\ tot}}\right)\left(\frac{\theta_{sym}=2\pi/3}{2\pi}\right)$
  - After the first propagation the renormalization is: $\mathrm{n_{cell}}\ [\mathrm{m^{-3}}] = \left(\sum_{all\ cells} n_{cell}\right)\left(\frac{N_{part\ cell}}{N_{part\ tot}}\right)\left(\frac{\theta_{sym}=2\pi/3}{2\pi}\right)$
  - The average energy in the cell is computed from the speed distributions

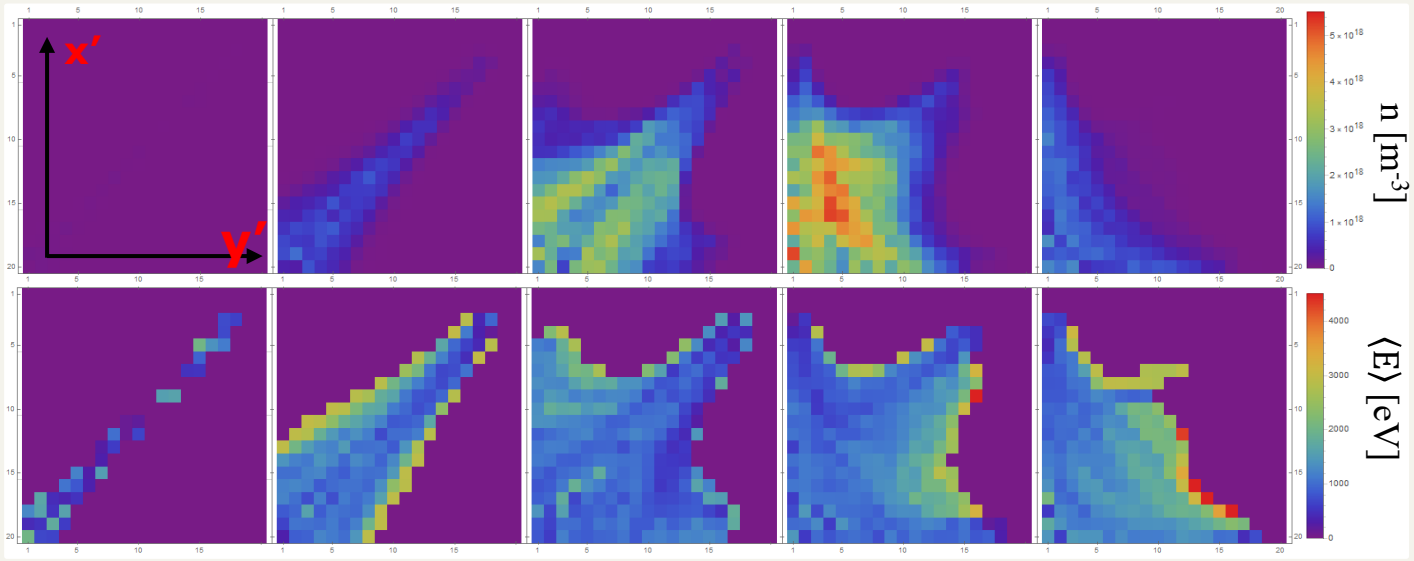

-MC ECR plasma simulation- Coulomb collisions

- The implementation of Coulomb scattering through a modified TA method produces a significant difference between the trajectories.
- The effect of coulomb scattering on the confinement of electrons was seen and qualitatively conforms with expectation.

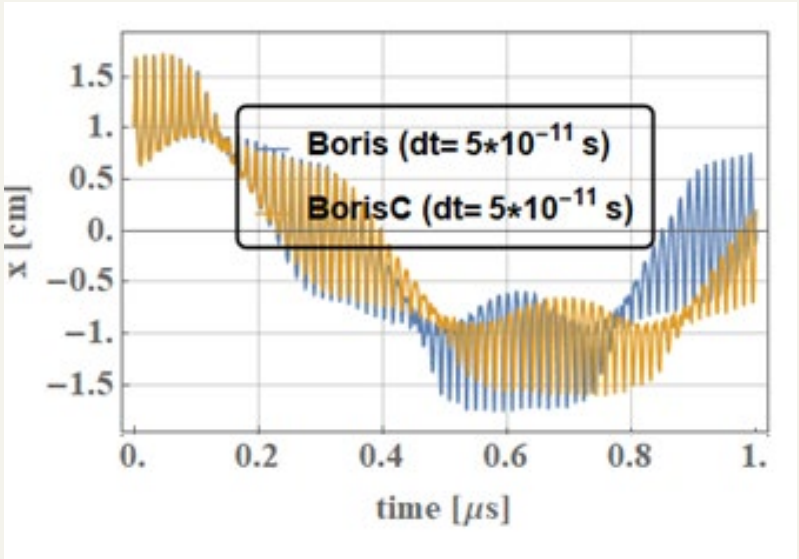

Sample orbit with and without Coulomb

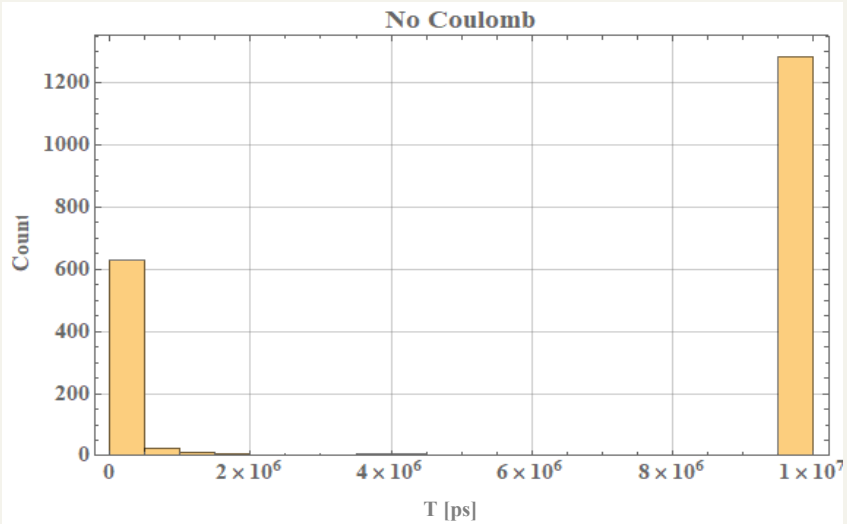

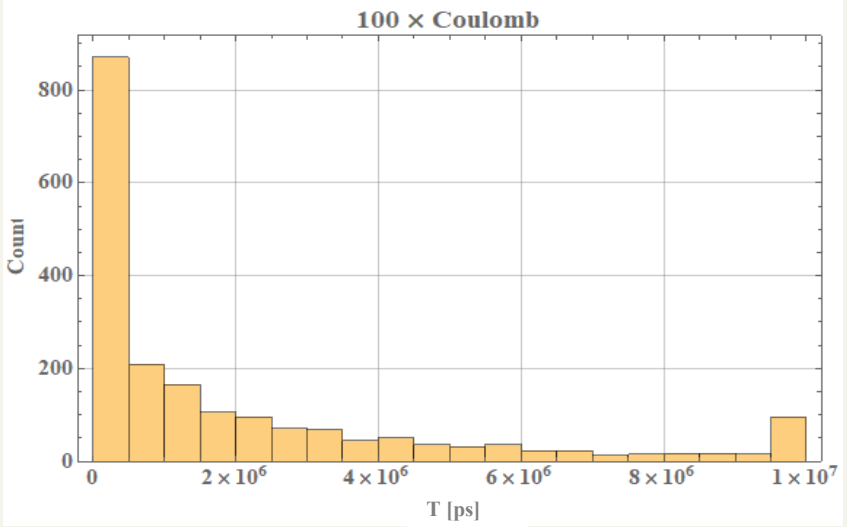

Confinement time (T) distribution for 2000 e-

-MC ECR plasma simulation- Inelastic collisions

- Handling through the null-collision method (work in progress)
  - Computing the probability of each interaction (P_i) can be avoided by choosing a constant collision frequency such that:

$$\nu' = \max_{\mathbf{x},\varepsilon}(v\sigma_T n_t) = \max_{\mathbf{x}}(n_t)\max_{\varepsilon}(v\sigma_T)$$

  - This corresponds to adding another collision, whose frequency, when added to the total collision frequency $\nu_i\sigma_T(\varepsilon_i)n_t(\mathbf{x}_i)$ is constant. This is called null collision as no interaction occurs.
  - The maximum ratio of particles of a species experiencing collisions is then:

$$P_{null} = 1 - \exp(-\nu'\Delta t)$$

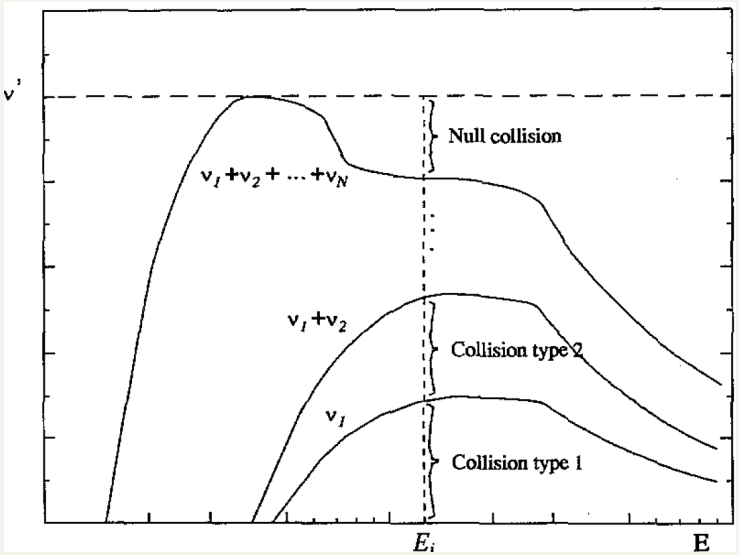

For a random number R [0,1]

$$R \leq \nu_1(\varepsilon_i)/\nu'$$
$$\nu_1(\varepsilon_i)/\nu' < R \leq (\nu_1(\varepsilon_i) + \nu_2(\varepsilon_i))/\nu'$$
$$\dots$$
$$\Sigma_{j=1}^{N}\nu_j(\varepsilon_i)/\nu' < R$$

-MC ECR plasma simulation- Relevant collision processes

$\sim\Delta t_{He1+He1+}$	4.89E-04 s	$\sim\nu_{He1+He1+}$	2.04E+03 Hz
$\sim\Delta t_{He1+He2+}$	2.45E-04 s	$\sim\nu_{He1+He2+}$	4.09E+03 Hz
$\sim\Delta t_{He2+He2+}$	6.11E-05 s	$\sim\nu_{He2+He2+}$	1.64E+04 Hz
$\sim\Delta t_{eHe1+}$	1.02E-03 s	$\sim\nu_{eHe1+}$	9.77E+02 Hz
$\sim\Delta t_{eHe2+}$	5.12E-04 s	$\sim\nu_{eHe2+}$	1.95E+03 Hz
$\sim\Delta t_{ee}$	1.02E-03 s	$\sim\nu_{ee}$	9.82E+02 Hz

Coulomb collisions handled by TA

λ_d (Only e-)	3.72E-04 m
λ_d (All, ion contribution non-negligible)	4.26366E-05 m
ln(Λ)	12.58518922

Debye length and Coulomb logarithm

- The Debye length informs the scale for the mesh. It needs to be comparable in order to be able to resolve the plasma sheath.

Process	Energy range [eV]	$\sim\nu_{max}$ [Hz]	Relevance for the propagation of the species: e^-	He^+	He^{2+}
e^- impact ionization of He	24.5874<E	112	yes	no	no
e^- impact ionization of He^{+1}	54.4178<E	801	yes	yes	no
e^- impact excitation of He 1s2	19.8196<E	37	yes	no	no
e^- impact excitation of He^+ 1s	40.8<E	1400	yes	no	no
e^- radiative recombination with He^{+1}	0<E	2.4	yes	yes	no
e^- radiative recombination with He^{+2}	0<E	27	yes	no	yes
single charge exchange He^{+1}+He	0<E	114	no	yes	no
single charge exchange He^{+2}+He	0<E	800	no	no	yes
double charge exchange He^{+2}+He	0<E	80	no	no	yes

Collisions handled by null-collision

- The relevance of a collision to a specific species propagation depends on if it affects the species status (dead or alive) or provides a considerable energy kick.
- The maximum collision frequency for the processes of interest was estimated in order to set the collision computation timestep (~100xcollision period)

BEAM TRANSPORT SIMULATION

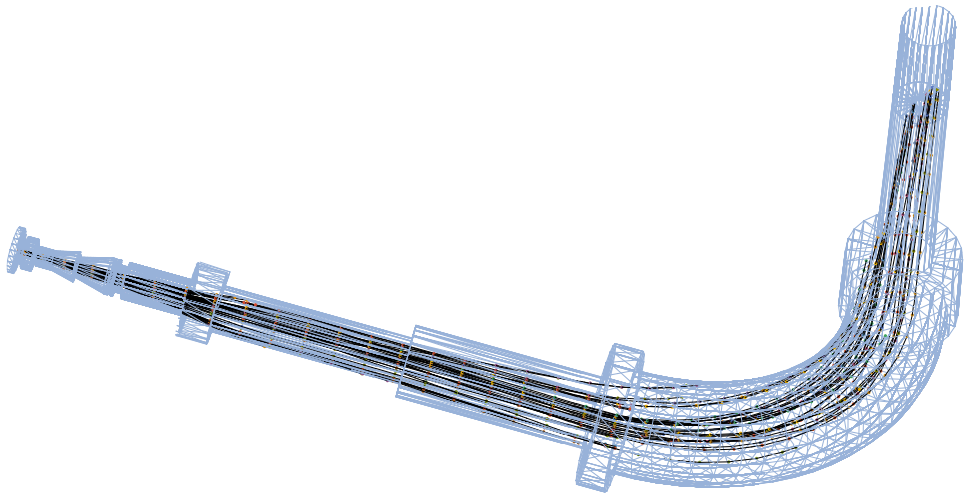

-Beam transport simulation- The LEBT

- The beam transport c code uses the Boris algorithm to propagate N macroparticles of a given species to achieve a set current at source extraction.
- Space charge effects are taken into account as well as residual gas neutralization (as a given parameter)
- Experimentally a transmission of 70% can be reached, not yet matched by the simulation, further development needed for physical results.
- Awaiting experimental results for further development of this module. (work-in-progress)

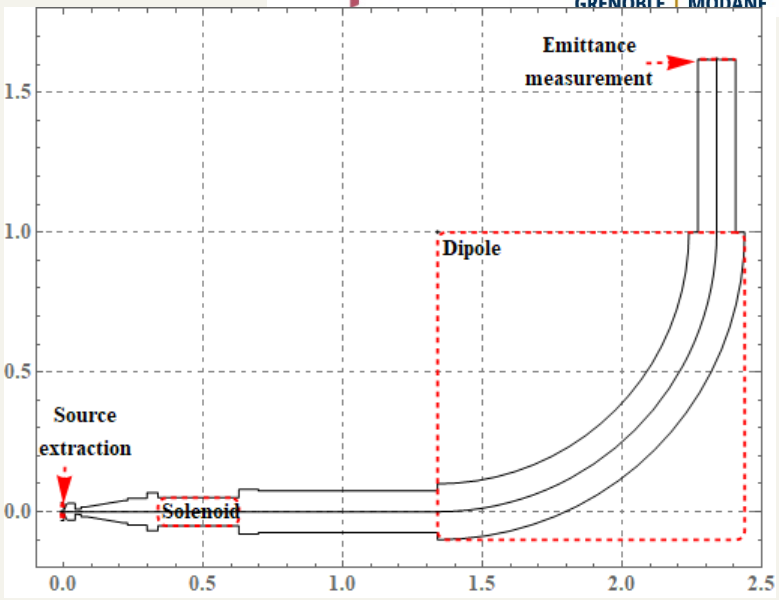

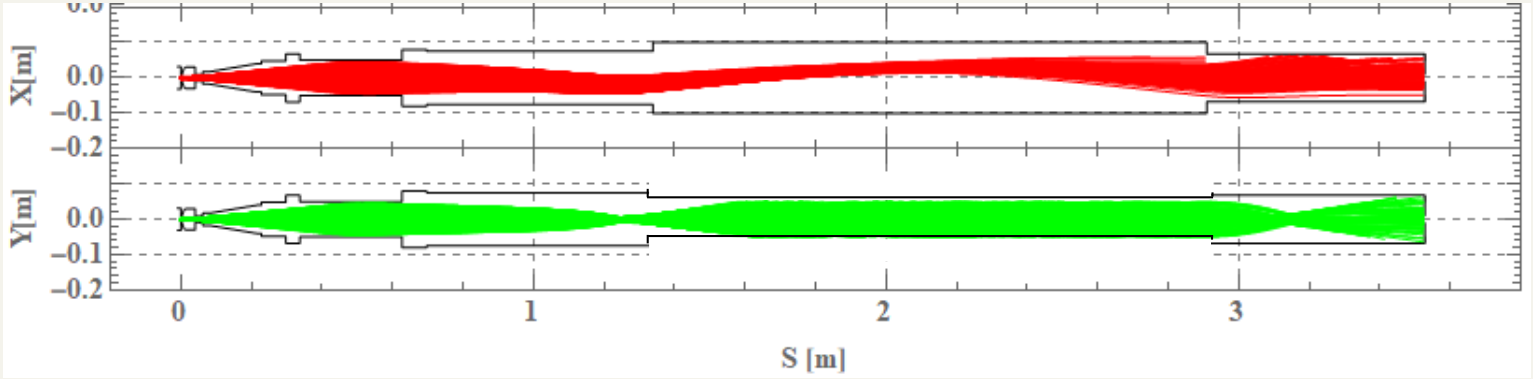

Simulated beam transport example for a He+ beam, I=4.mA

-Beam transport simulation- The LEBT & Components

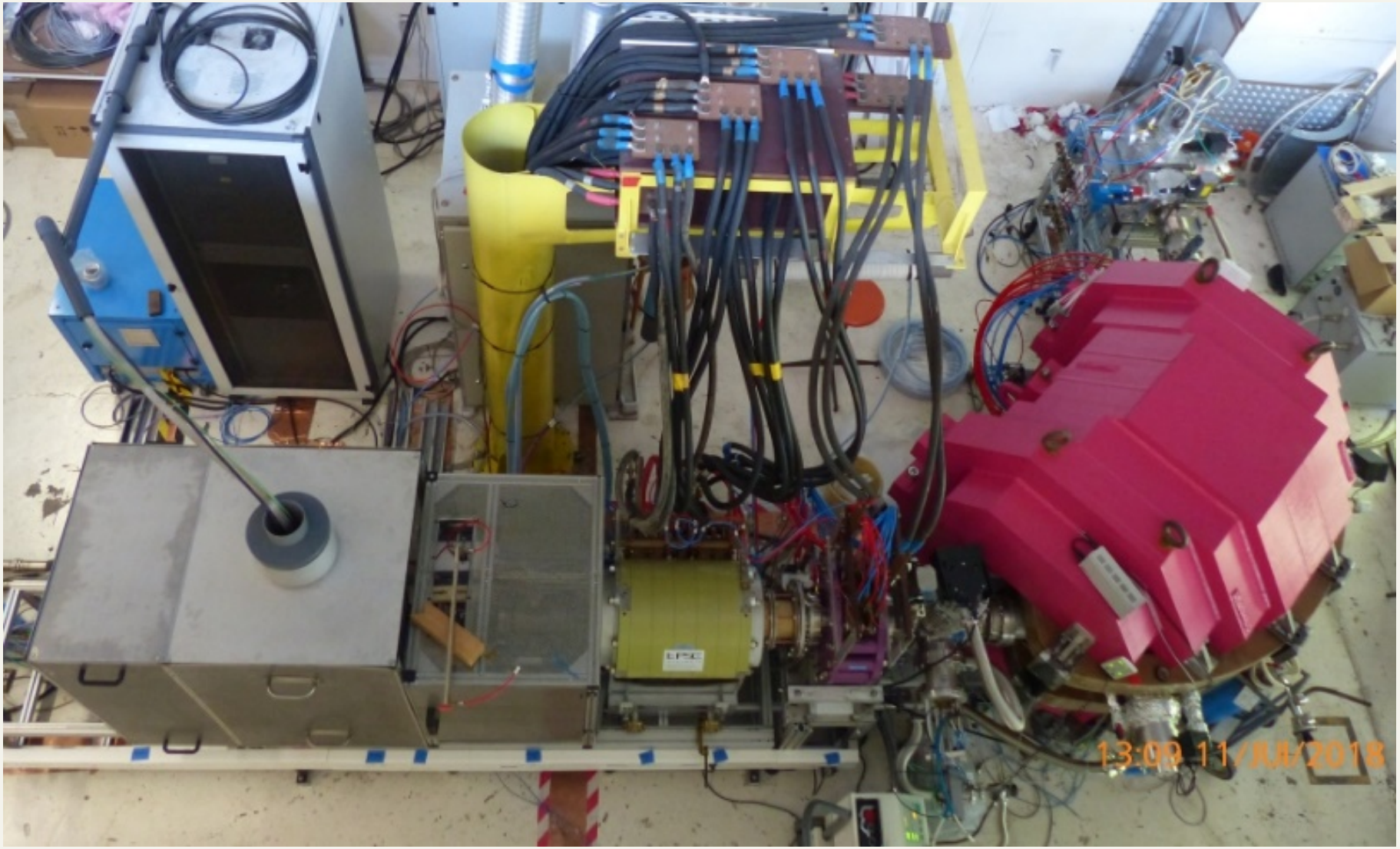

-Beam transport simulation- The LEBT & Compon

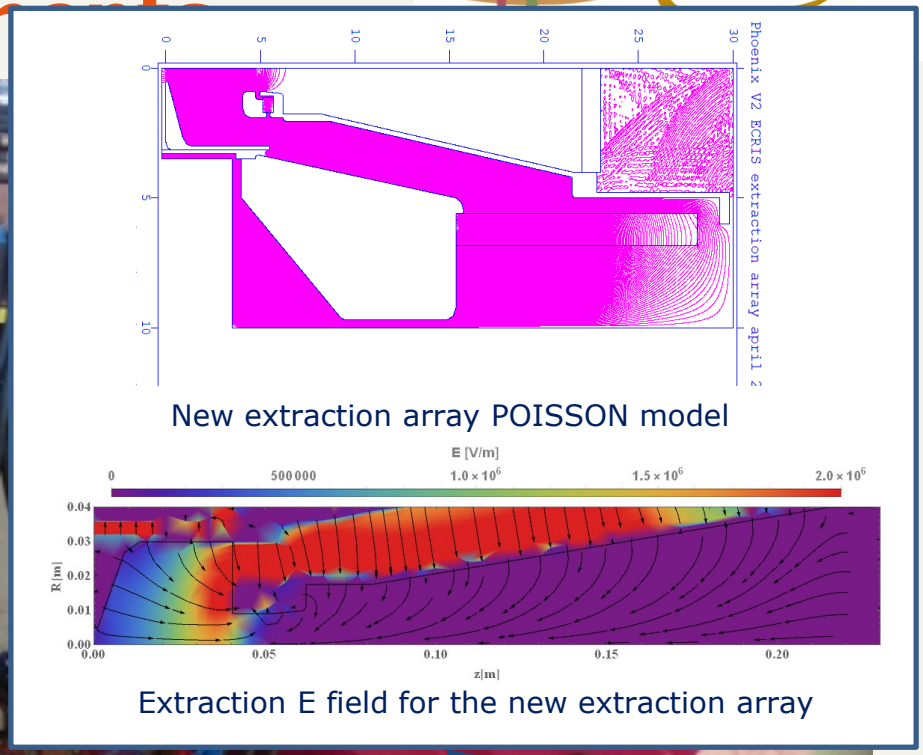

New extraction array POISSON model

Extraction E field for the new extraction array

-Beam transport simulation-
The LEBT & Compo

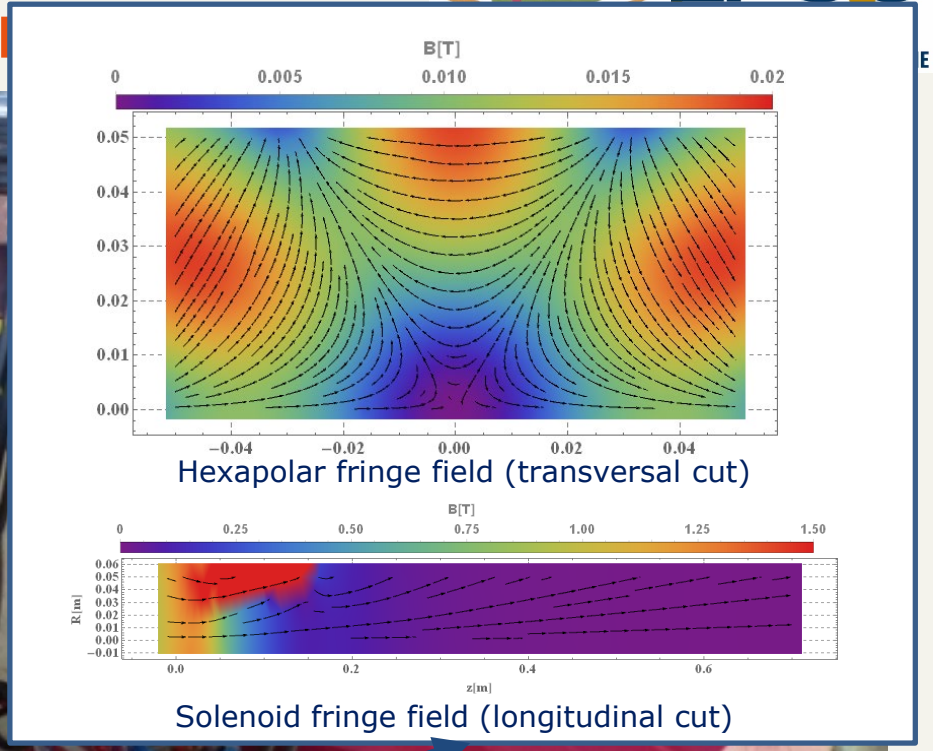

Hexapolar fringe field (transversal cut)

Solenoid fringe field (longitudinal cut)

-Beam transport simulation-

nents

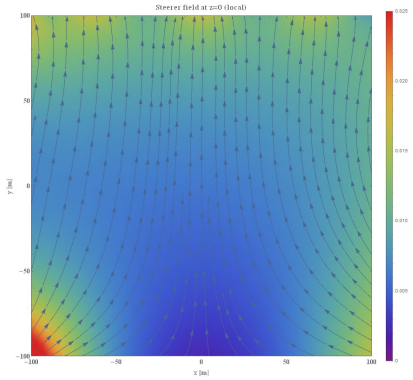

Steerer field against (transversal cut)

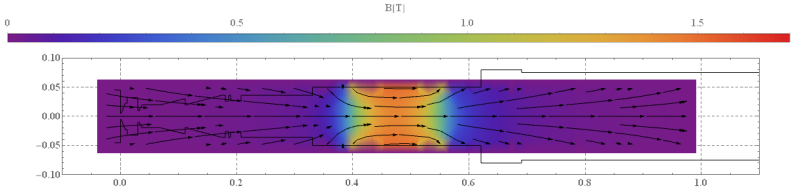

Focusing solenoid's magnetic field in the Z, R plane

-Beam transport simulation-

nents

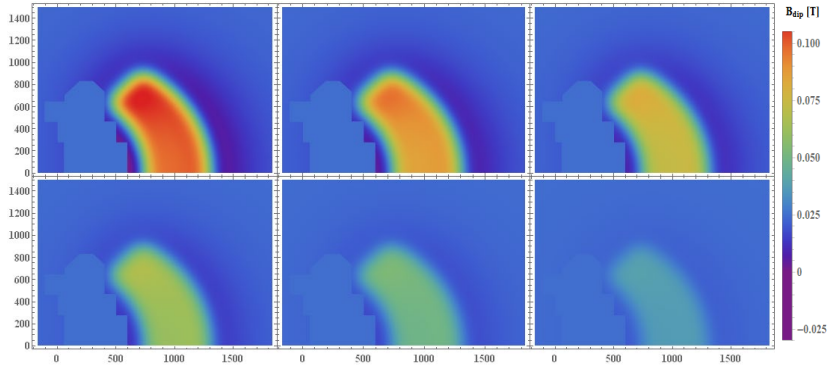

Vertical dipole magnetic field at the centre plane for j=0.4, 0.8, 0.12, 0.16, 0.20, 0.24 A/mm^2

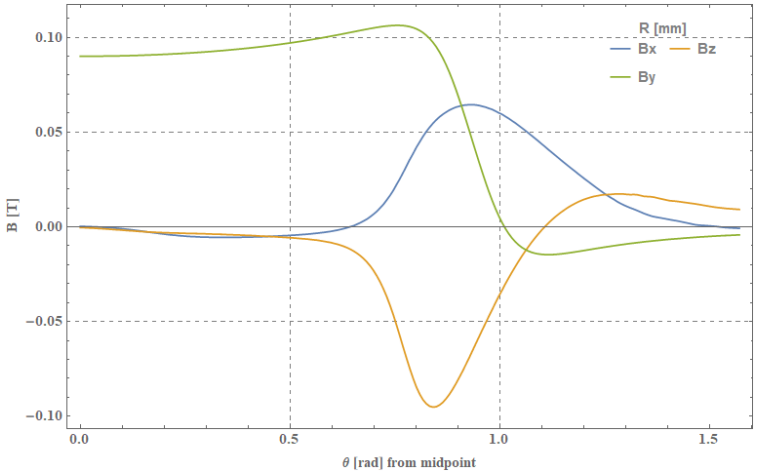

Dipole field at $j = 0.24\ A/mm^2$ from Opera 3D simulation

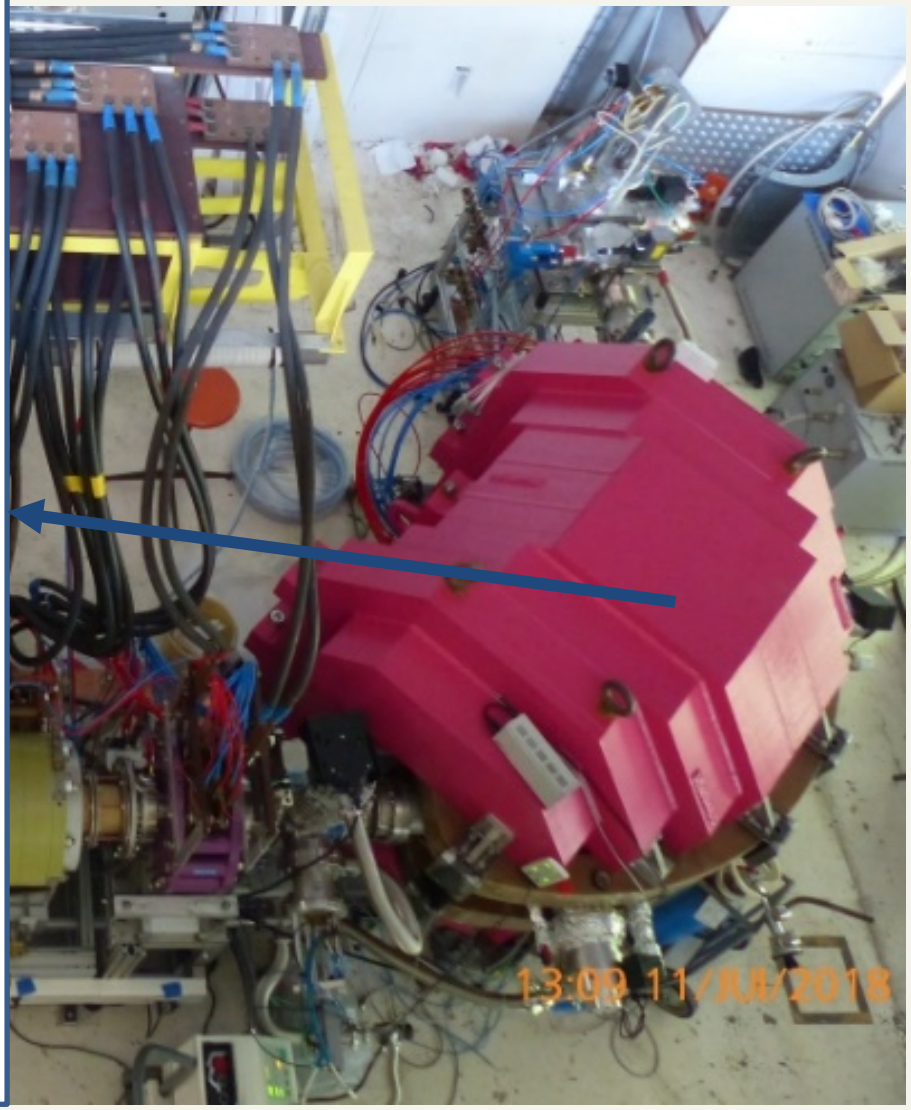

-Beam transport simulation-

nents

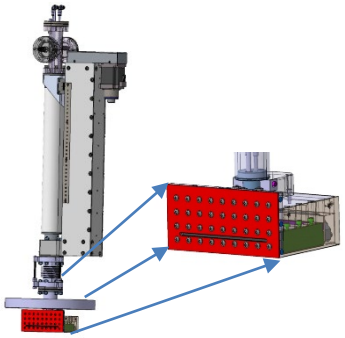

Future Allison emittancemeter CAD

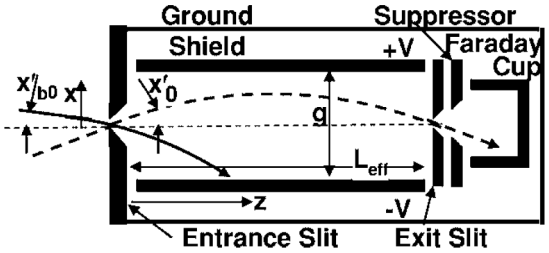

Allison type emittance scanner schema

CONCLUSIONS & PROSPECTS

-Conclusions & Prospects-

Conclusions

- Studying plasma, ion beam formation and beam propagation simulation for ECR ion sources is an area of great intertest, especially in terms of aiding their design and development.
- The GC algorithm can provide an advantage in terms of computation time for particle plasma simulations. For the Phoenix V2 ECRIS the gains are significant, with a time-step increased by a factor of 10^2 and one order of magnitude gain in computation time.
- The novel MC approach for the simulation of ECR Plasma is so far promising in terms of providing a relatively light-weight framework for this type of plasma characterization.

Prospects

- (simu) Implement inelastic collisions, Poisson solving, microwave heating and neutral diffusion, and consolidate the ECR Plasma Monte-Carlo simulation into the higher order loop for density and energy species distributions convergence.
- (simu) Adapt the ONIX PIC beam extraction code (LPGP) to the extraction array of PHOENIX V2 and propagate the extracted beam in the simulated LEBT.
- (exp) Install the Allison type emittance scanners, and the faraday cup beam dump on the LEBT on the "Banc Fort Courant" test bench (LPSC).
- (exp) Validate the beam characterization (current, energy, emittance) results by experimental measurements of the beam along the LEBT.

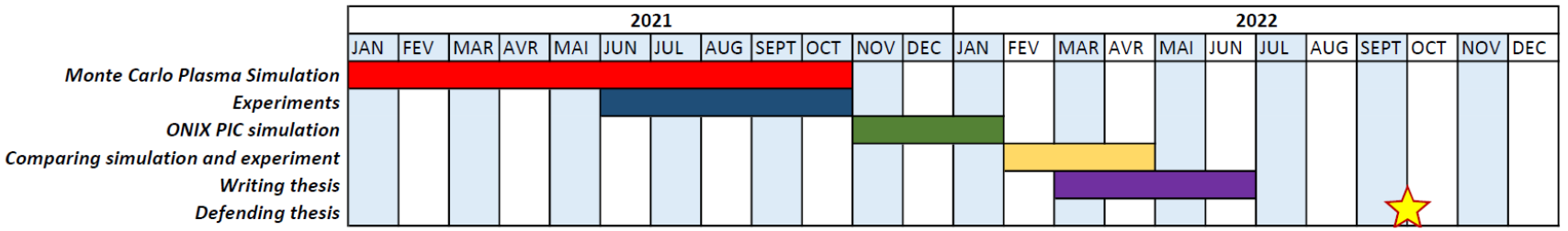

THANK YOU FOR LISTENING!

APPENDIX

-Introduction-
Phoenix V2 min-B field

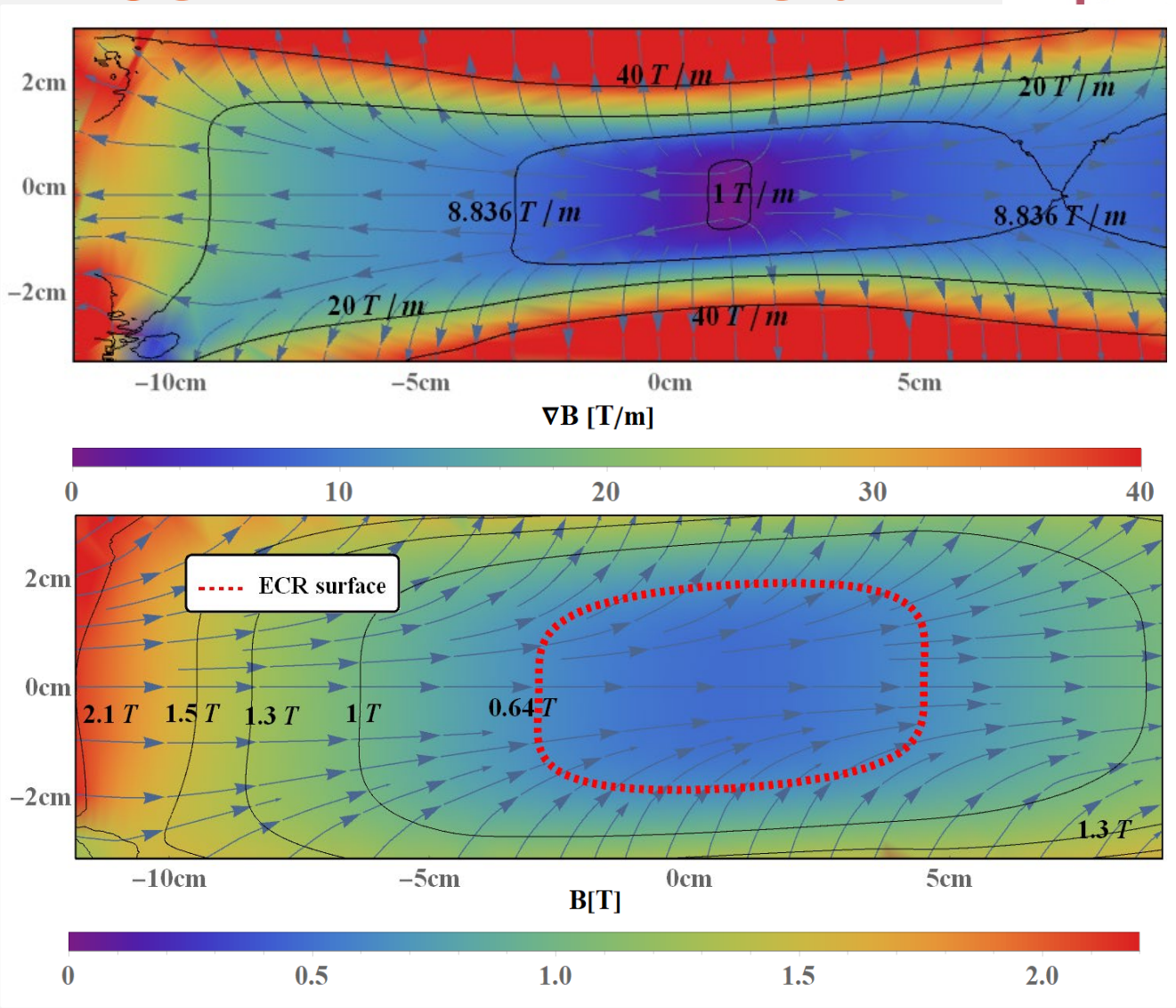

Figure: Phoenix V2 magnetic field and it's gradient, longitudinal cross section map

-Beam transport simulation- Magnets: Source's fringe fields

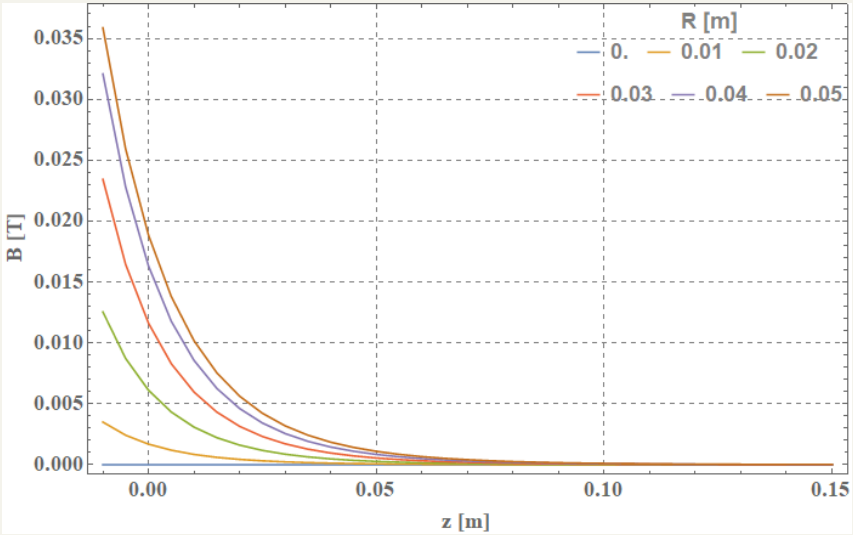

Hexapole's fringe field at various R

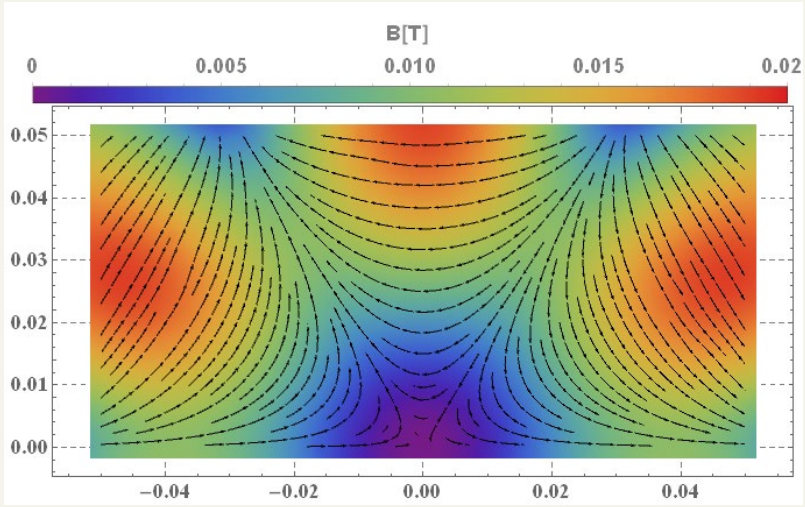

- RADIA (ESRF), used for the magnet modelling

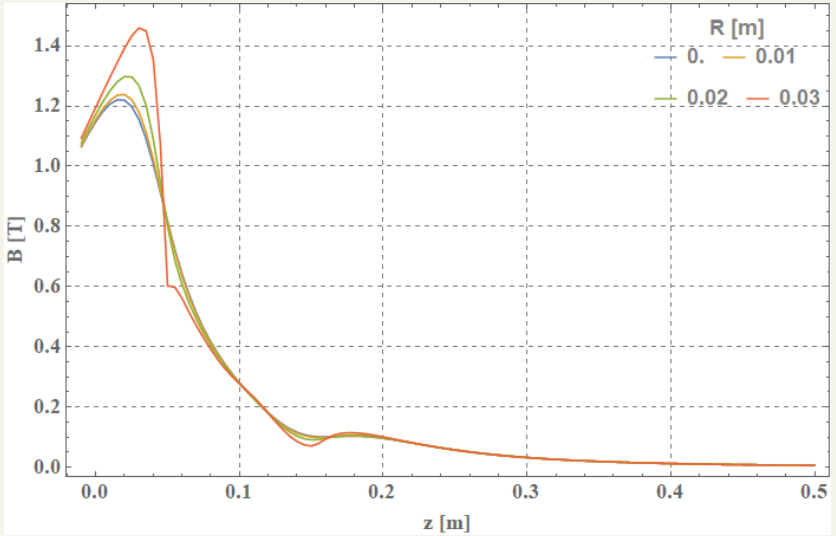

Solenoid's fringe field at various R

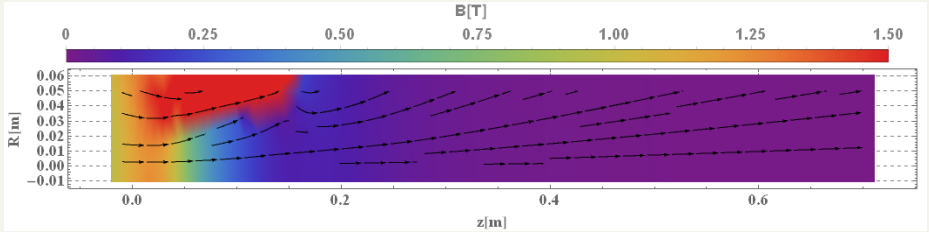

- The Solenoid's fringe field plays an important role at extraction at it provides a focusing effect

-Beam transport simulation- Magnets: solenoid & steerer

- In order to keep the beam focused through the first straight section of the LEBT and adapt it to the dipole's aperture, a focusing solenoid and steerer are employed

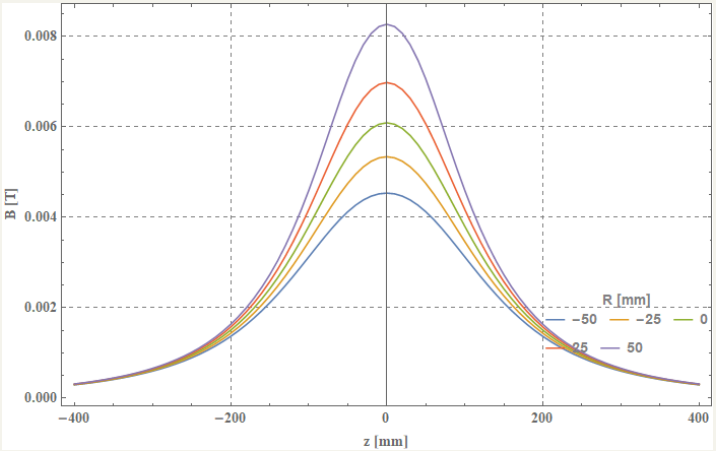

Steerer field against z [mm]

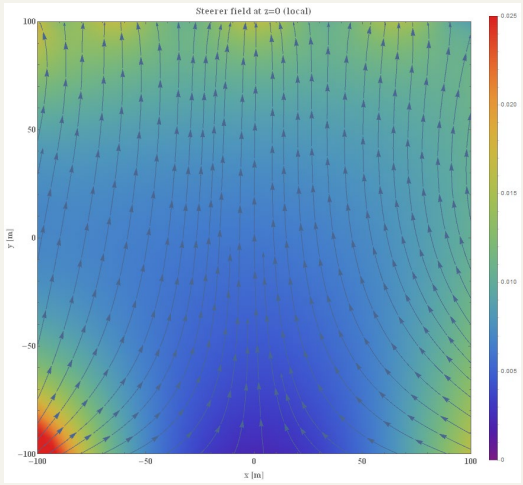

Steerer field against X, Y plane

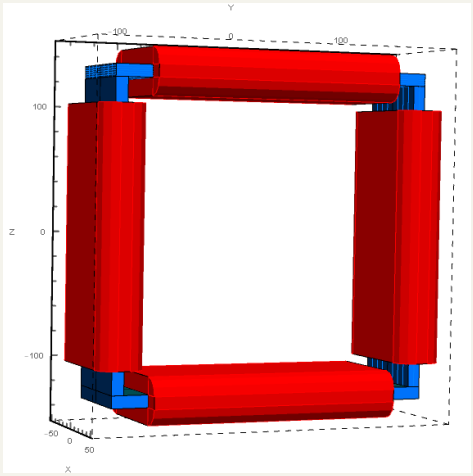

Steerer model

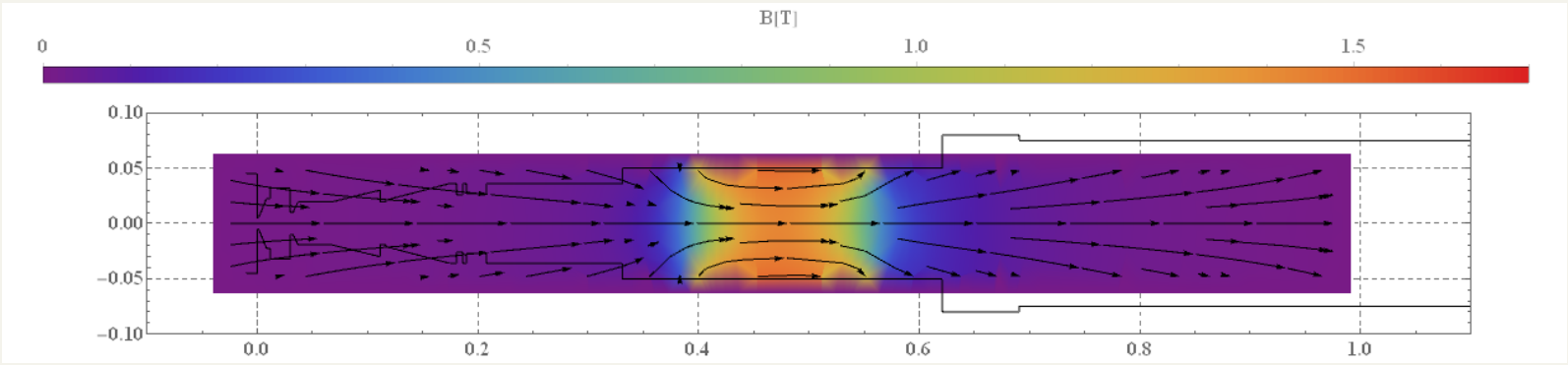

Focusing solenoid's magnetic field in the Z, R plane

Beam transport simulation
Dipole saturation

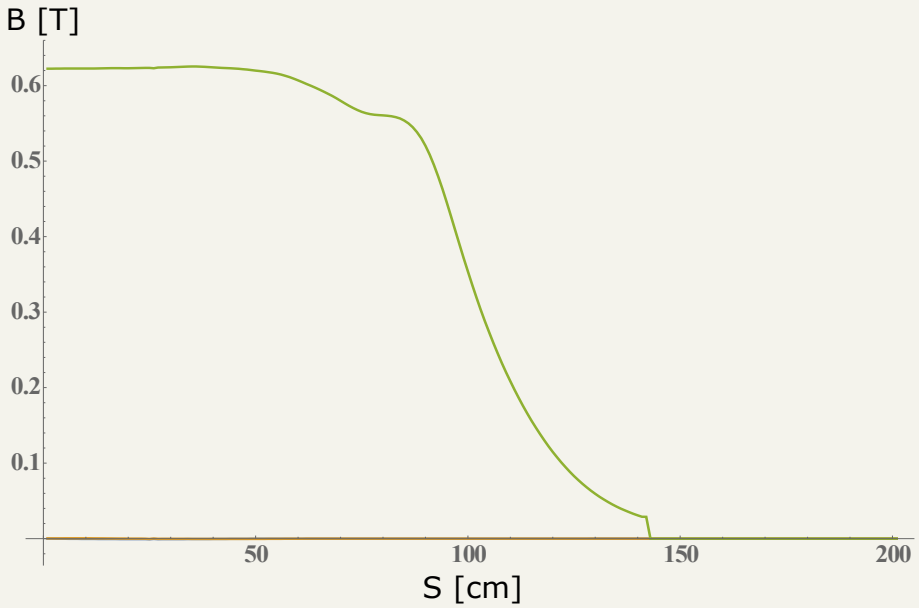

Dipole field at saturation from Radia (ESRF) simulation.

- The DI3 dipole reaches a 0.6T vertical magnetic field at saturation. This is very high for the LEBT's energy range.
- At saturation the vertical (Y) field greatly dominates the other components, failing to provide the fringe field's focusing effect.

-Beam transport simulation- Magnets: DI3 Dipole

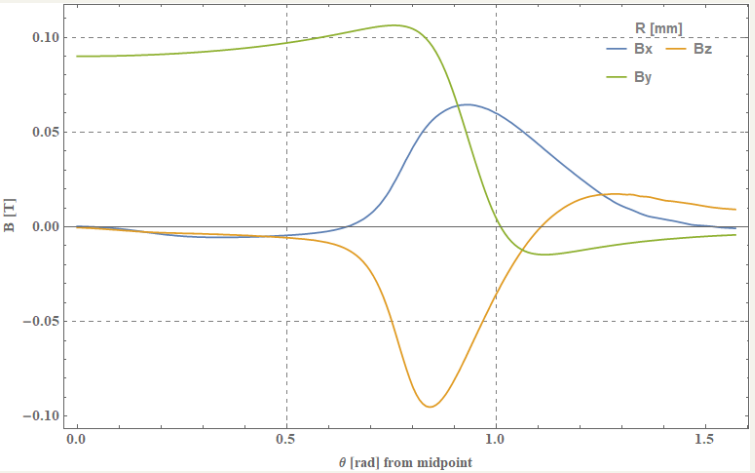

Dipole field at $j = 0.24\ A/mm^2$ from Opera 3D simulation

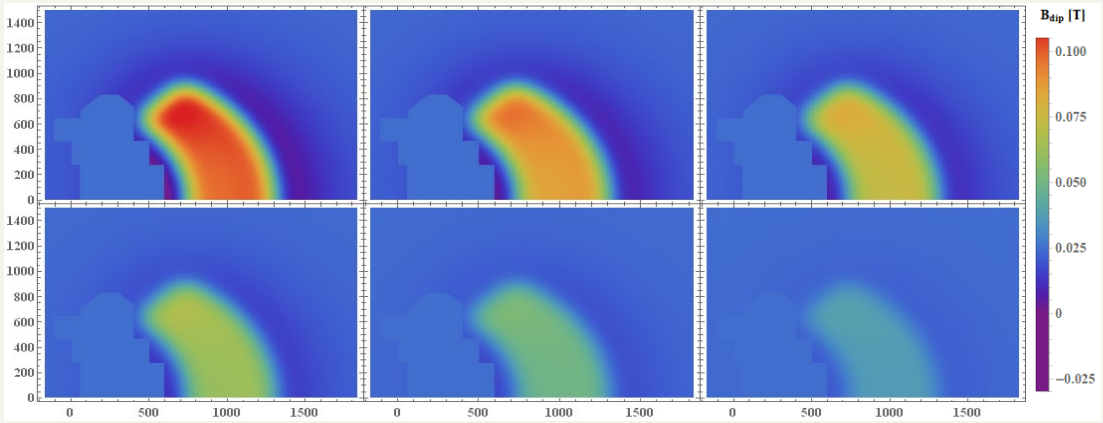

Vertical dipole magnetic field at the centre plane for $j = 0.4,\ 0.8,\ 0.12,\ 0.16, 0.20, 0.24\ A/mm^2$

- OPERA 3D is a commercial electromagnetic simulation software, it uses the finite element method
- It is able to converge to a solution for the dipole magnetic field even far from saturation.
- The DI3 dipole reaches a nominal field of 0.6T at saturation and has a bending radius of 1m.
- DI3 is a high energy dipole refurbished from the former LPSC cyclotron accelerator. In the LEBT it is used at very low current (B=0.03T)

-Beam transport simulation- Extraction array

- A newly designed extraction array was modelled

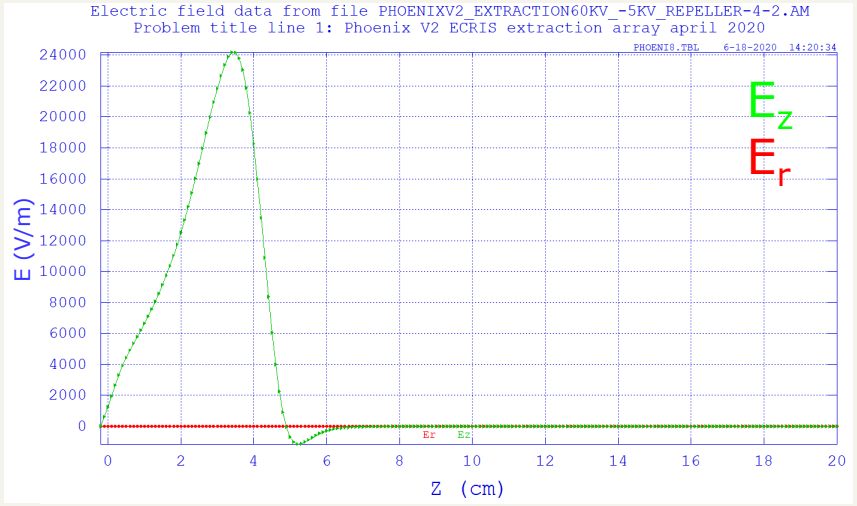

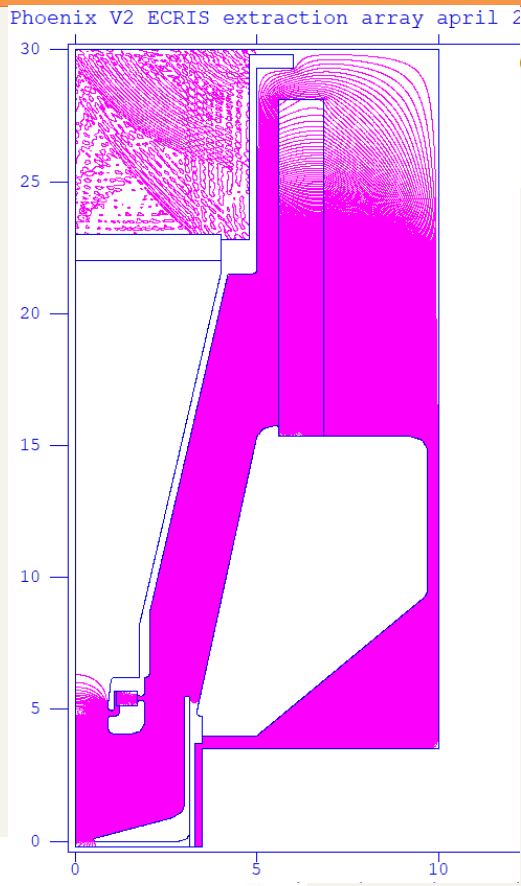

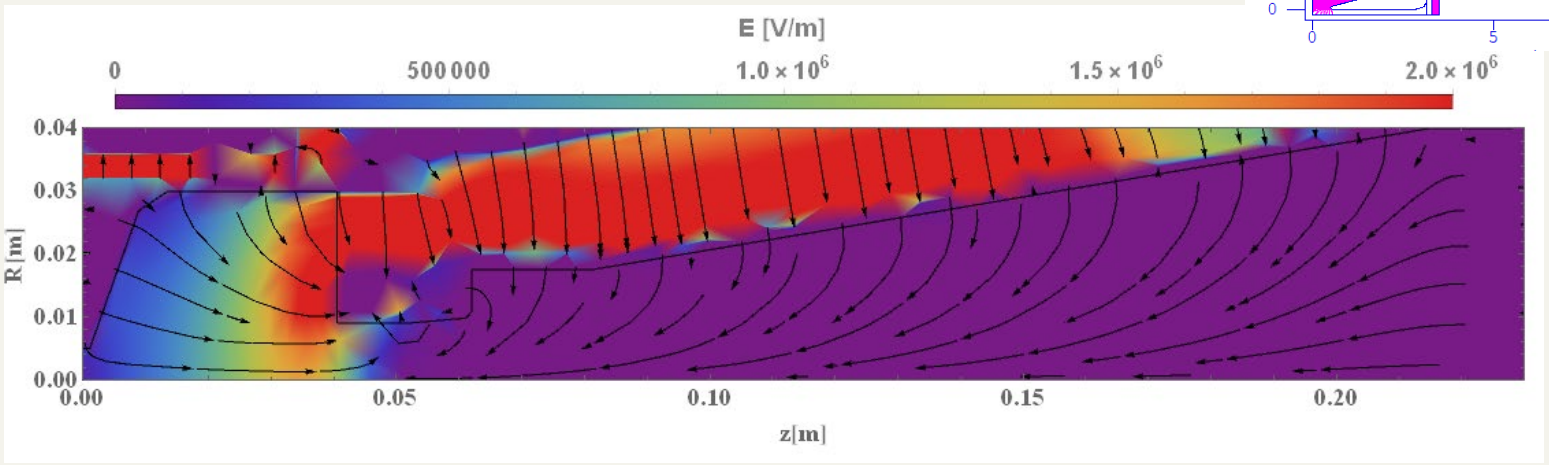

Extraction E field for the new extraction array

Beam transport simulation
Space charge compensation

- $z < Z_{neutr}$: $T_{neutr} = e^{\frac{V(\vec{r})-V_{max}-V_p}{T_e}}$ -> only sheath electron density contribution
- $z > Z_{neutr}$: $T_{neutr} = e^{\frac{V(\vec{r})-V_{max}-V_p}{T_e}} \left(1 - \left(1 + e^{-\frac{z^2-Z_{neutr}^2}{r_{extr}^2}}\right)^{-1}\right) + T_{neutr}^0 \left(1 + e^{-\frac{z^2-Z_{neutr}^2}{r_{extr}^2}}\right)^{-1}$

T_{neutr}^0: constant space charge compensation rate (interaction with neutral residual gas)

Z_{neutr}: user defined source electron effect range (end of extraction potential gradient)

- Taking the electron density to follow a Boltzmann distribution, true under thermal equilibrium.
- The neutralization factor is applied at each step to the macroparticle (MP) charge (NOT ion charge)
- The space charge force for each macroparticle is computed by taking the effect of all MP closer to the axis as a point charge at their centre of mass with their combined MP charge.
- The ionization ratio tends fast to the fixed value (T_{neutr}^0) after defined Z_{neutr}(=20cm), typically 0.8, observed to replicate experimental measurements in simulation.
- The effects of space charge are clearly visible in the resulting ion track at I > 2mA.
- The force is added to the electric field contribution on the Boris propagation algorithm.

-Beam transport simulation- Transmission Optimization

- The relationship between many of the LEBT's components contribute to optimum beam transport.
  - When dealing with the simulated extracted He+, He2+ beam this relationships are to be determined and considered.

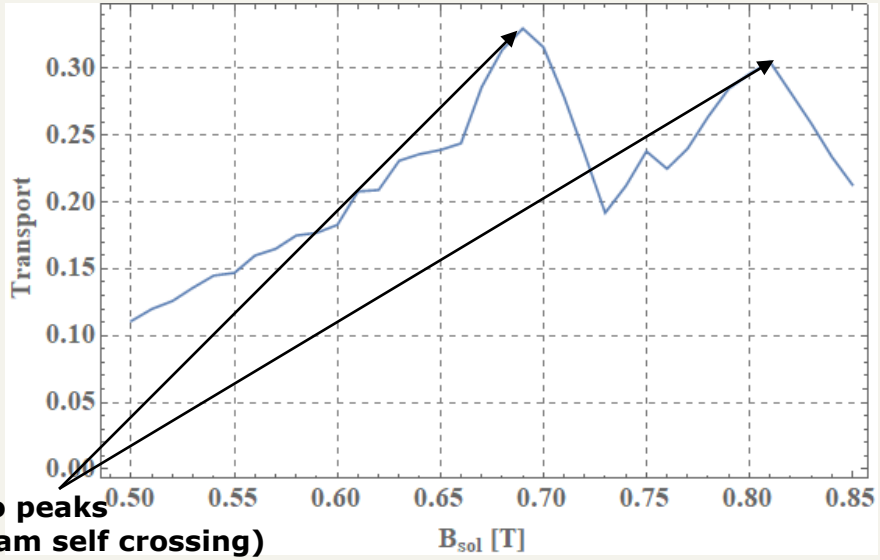

Two peaks (beam self crossing)

Transport vs solenoid's maximum B field

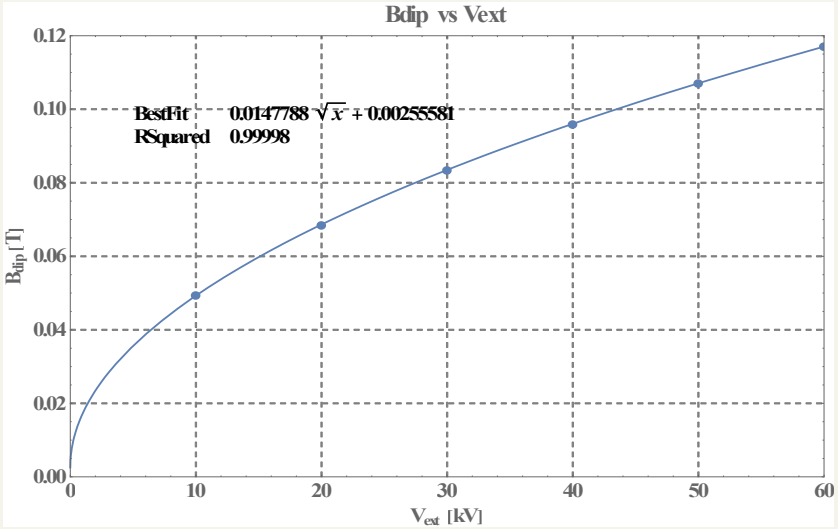

Dipole's nominal magnetic field vs extraction potential at the source's exit for reaching the emittance scanners

$$R = B\rho = \frac{mv_{\perp}}{Ze} = \sqrt{\frac{2mV}{Ze}}$$

Beam's magnetic rigidity corroborates this relationship

GC particle pusher Implementation

LPSC GRENOBLE | MODANE

General initialization

- Number of electrons, maximum propagation time and time-step are given
- Read provided magnetic field map files, merge them into a 3D grid.
- Set electrons' position ($\mathbf{r}$) (uniform disc) and velocity ($\mathbf{u} = \gamma\mathbf{v}$) (Maxwell-Boltzmann)

GC initialization

- Map ∇B (speeds up the computation per step without loss of accuracy)
- For each electron:
  - $u_{\parallel} = \boldsymbol{u} \cdot \hat{b}$
  - $\mathbf{R} = \mathbf{r} + \boldsymbol{\rho}$
  - Compute magnetic moment μ

Boris Algorithm

dt

GC Approximation

dt

- $\frac{d\mathbf{R}}{dt}$ and $\frac{du_{\parallel}}{dt}$ integrated concurrently by RK4

Output

- Track file (r, u, μ (GC), n_e, ε, t, t_{cpu})

GC particle pusher Boris algorithm

- The standard for magnetised plasma simulations.
- Second order, explicit method. Energy conserving while only a magnetic field is present.
- For B= 1T, $T_B=1/\omega_B \sim 35ps$ → $dt \sim 3ps$.

$$\frac{\mathbf{u}^{n+1}-\mathbf{u}^{n}}{\Delta t}=\underbrace{\frac{q}{m}\left(\mathbf{E}(\mathbf{x}^{n+\frac{1}{2}})+\left(\frac{\mathbf{u}^{n+1}+\mathbf{u}^{n}}{2\gamma^{n+\frac{1}{2}}}\right)\times\mathbf{B}(\mathbf{x}^{n+\frac{1}{2}})\right)}_{\text{Discretised Lorentz force with: } \bar{\mathbf{v}}=(\mathbf{u}^{n+1}+\mathbf{u}^{n})/2\gamma^{n+\frac{1}{2}}}\Rightarrow$$

$$\mathbf{u}^{-}=\mathbf{u}^{n}+\frac{q\Delta t}{2m}\mathbf{E}(\mathbf{x}^{n+\frac{1}{2}})$$

$$\mathbf{u}^{+}=\mathbf{u}^{-}+(\mathbf{u}^{-}+(\mathbf{u}^{-}\times\mathbf{t}))\times\mathbf{s}$$

$$\mathbf{u}^{n+1}=\mathbf{u}^{+}+\frac{q\Delta t}{2m}\mathbf{E}(\mathbf{x}^{n+\frac{1}{2}})$$

with: $\underbrace{\mathbf{u}^{n}=\mathbf{u}(t^{n}-\Delta t/2)=\gamma^{n}\,\mathbf{v}(t^{n}-\Delta t/2)}_{\text{Proper velocity}}$ and $\underbrace{\Delta t=\frac{2\pi m_e[eV]}{c^2 B_{min}\ \mathrm{Np}}}_{\text{time-step } T_{Bmin}/\mathrm{Np}}$

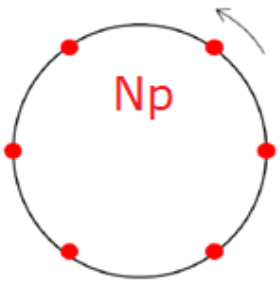

Np is the number of points to calculate per orbit at B_{min}

-GC particle pusher-
ECR orbit Far From Axis (FFA)

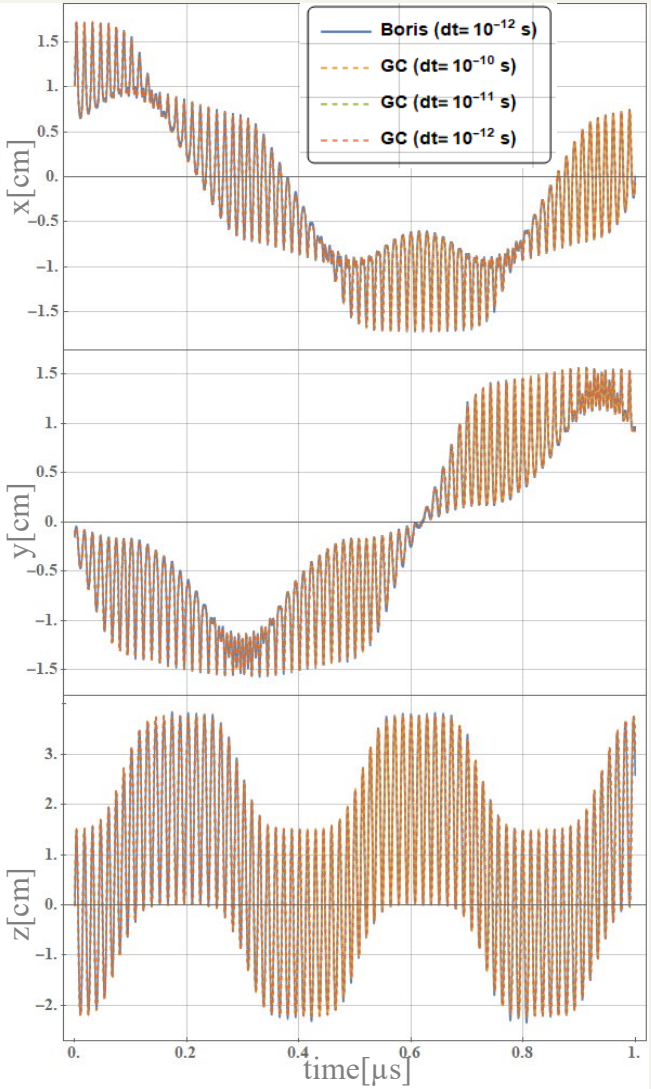

Confined electron orbit components

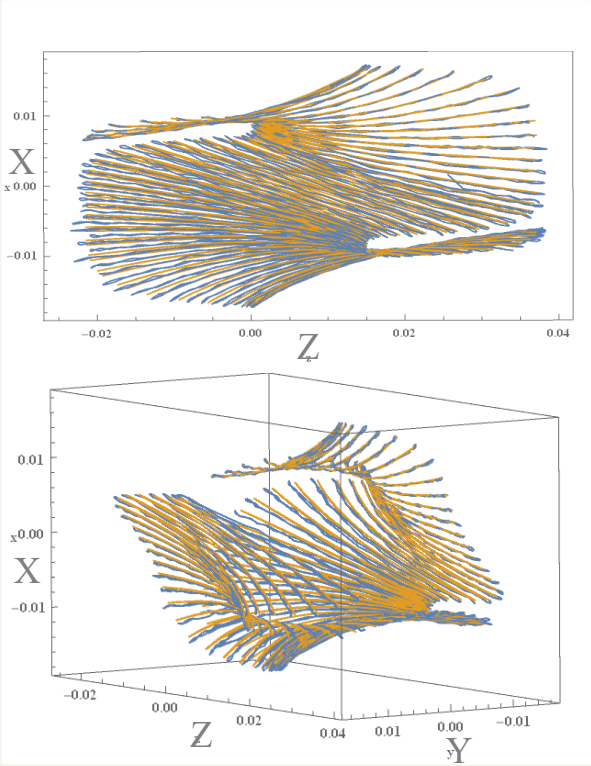

Confined electron orbit 3D plot

- Good agreement between Boris and GC with ~1μs of propagation.

GC particle pusher
ECR orbit Close To Axis (CTA)

- Disphasement observed between the GC and Boris orbits
- Spatial envelopes are consistent.

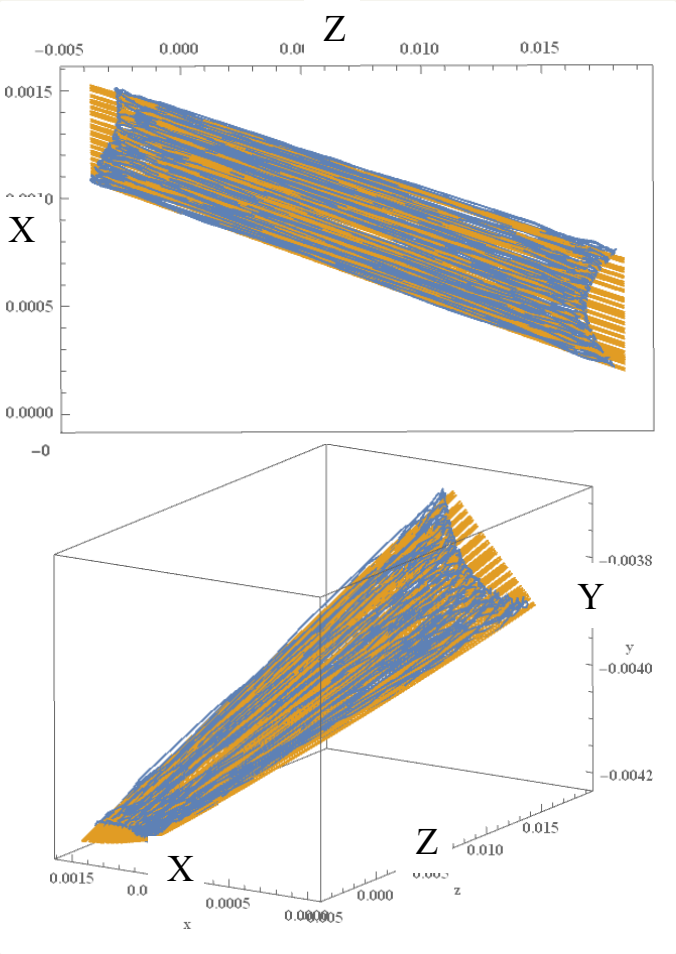

Figure: Confined electron orbit 3D plot

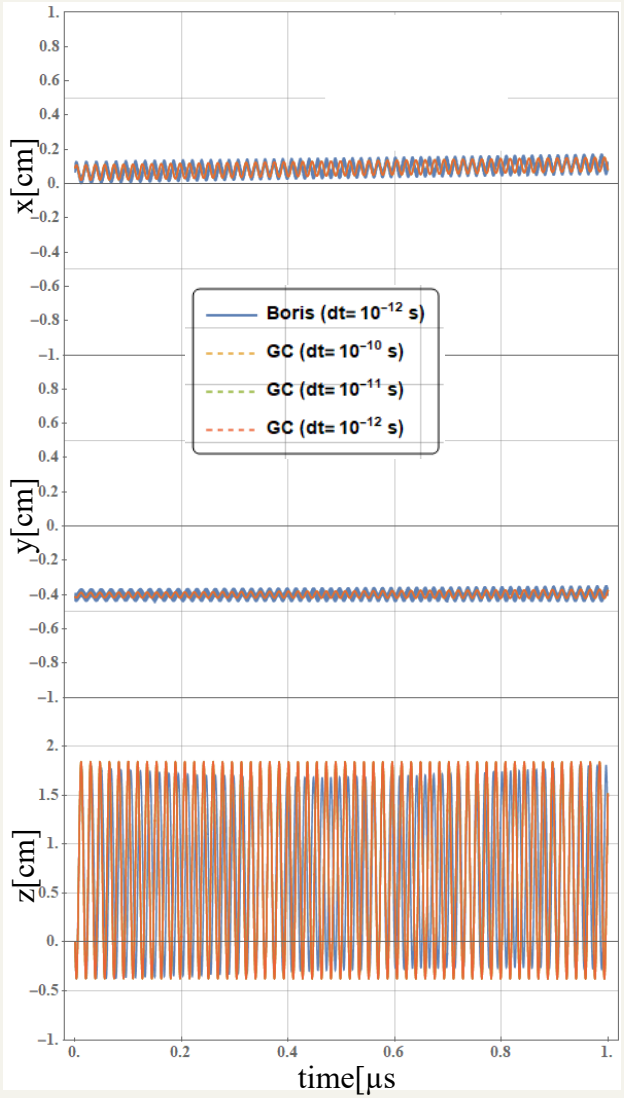

Figure: Confined electron orbit components

GC particle pusher
ECR orbit analysis (CTA)

- The observed disphasement is evident
- Good agreement between Boris and GC
- This orbit is one of the hardest for GC, (high axial oscillation frequency)
- Stable at this time-scale

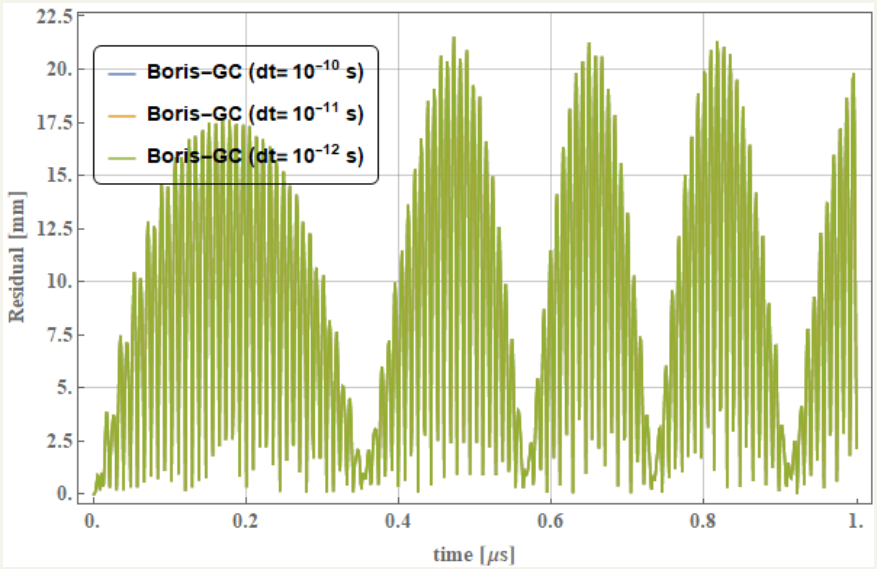

Figure: Boris-GC orbit residual at corresponding propagation times.

Energy conserved with both methods

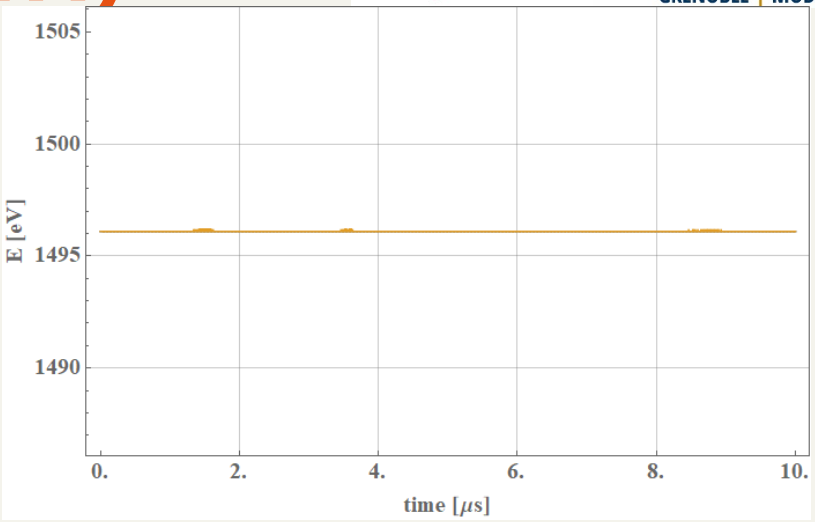

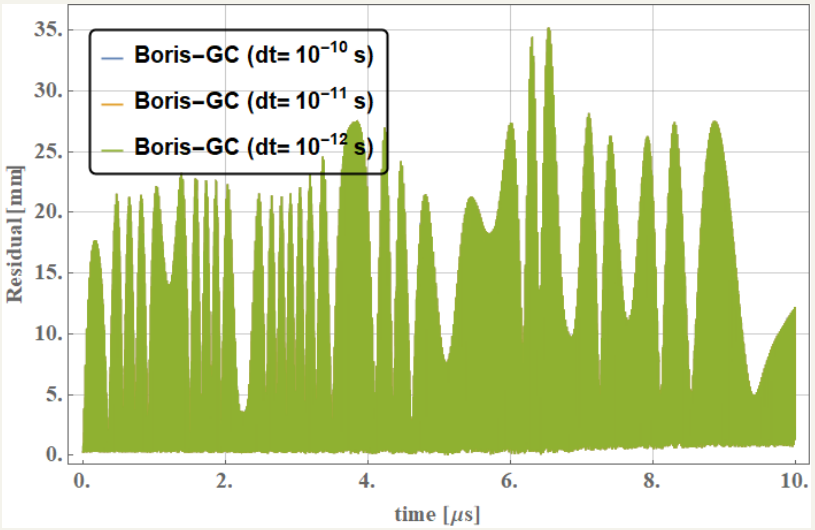

Figure: Boris-GC orbit residual at corresponding propagation times.

GC particle pusher SILHI@GANIL ion source

- 2.45GHz operation frequency
- Microwave discharge ion source (MW)
- ~0.1T maximum solenoidal magnetic field. (2D map given)
- No magnetic confinement, one magnetic mirror towards extraction

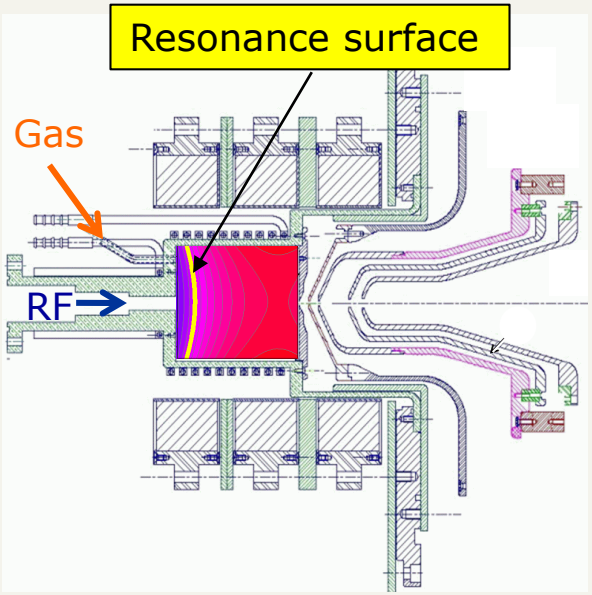

Figure: SILHI source with permanent magnets (CEA/IRFU/GANIL)

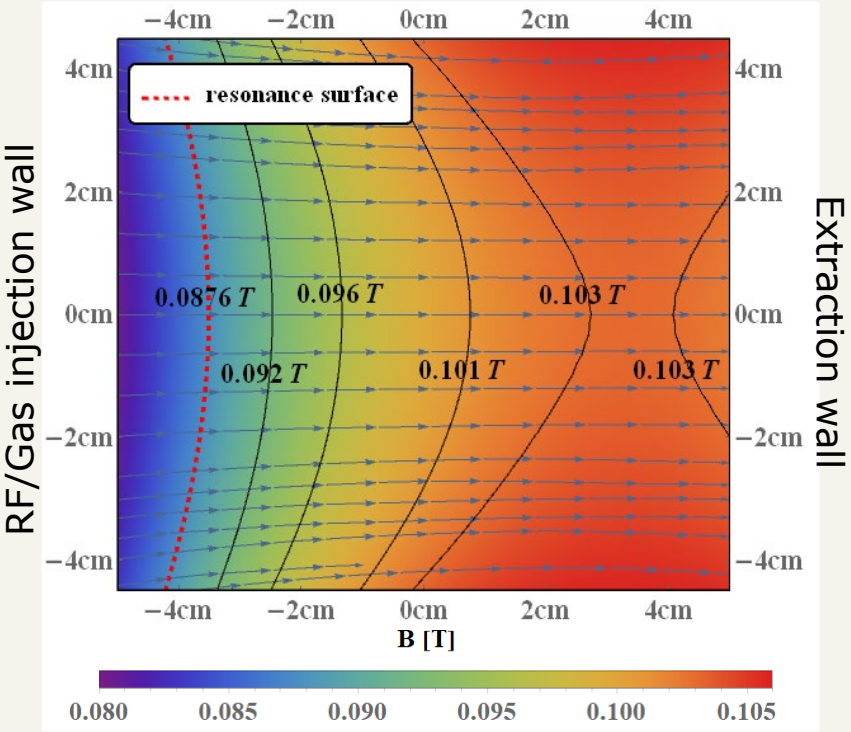

GC particle pusher
SILHI B field and gradient

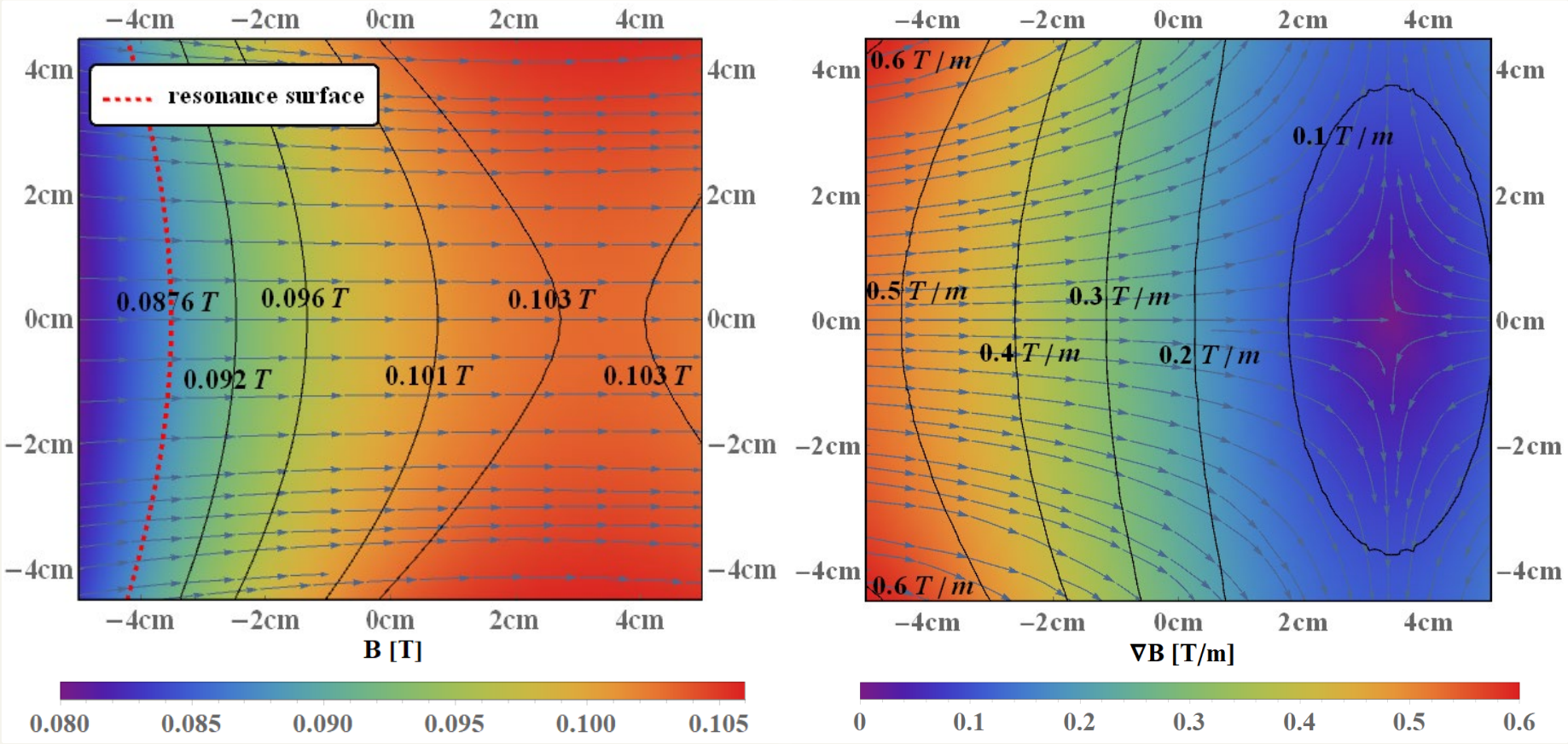

GC particle pusher
Trapped orbit in SILHI (1 bounce)

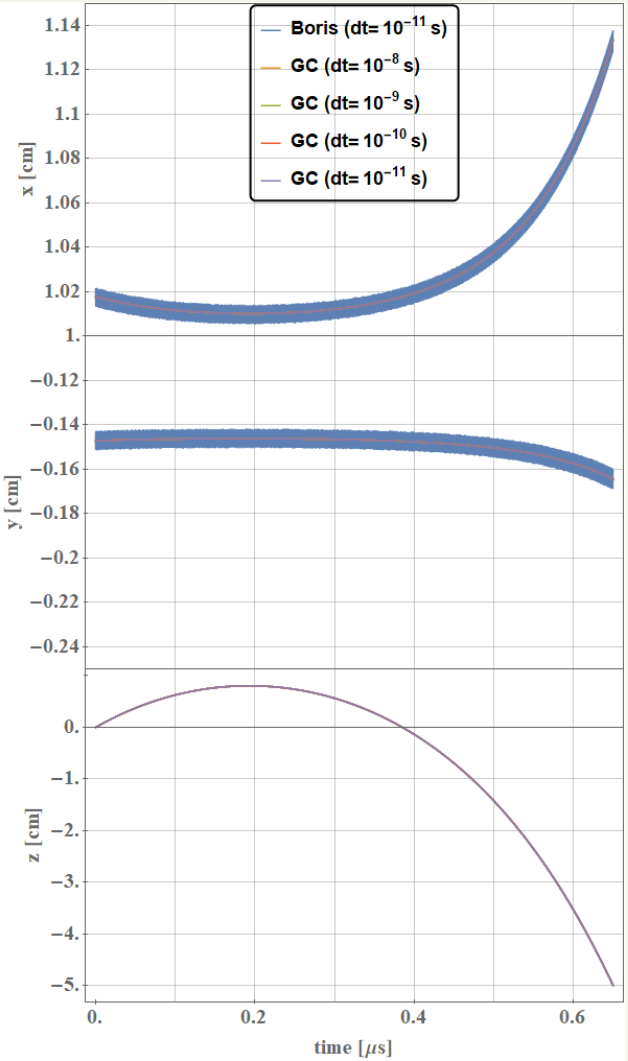

- Very good qualitative agreement.
- A one bounce orbit chosen as it is one of the most challenging examples.
- A typical energy electron of ~1eV is confined for ~1μs. In the absence of interaction

Figure: One bounce electron orbit components

GC particle pusher
Trapped orbit analysis

- GC algorithm ~5.7 times more computationally expensive per step.
- 10 times larger timestep rends it faster.
- The GC trajectories stable up to a 1000ps time-step, broken at a 10^4ps.
  - GC up to ~10 times faster when compared to Boris.

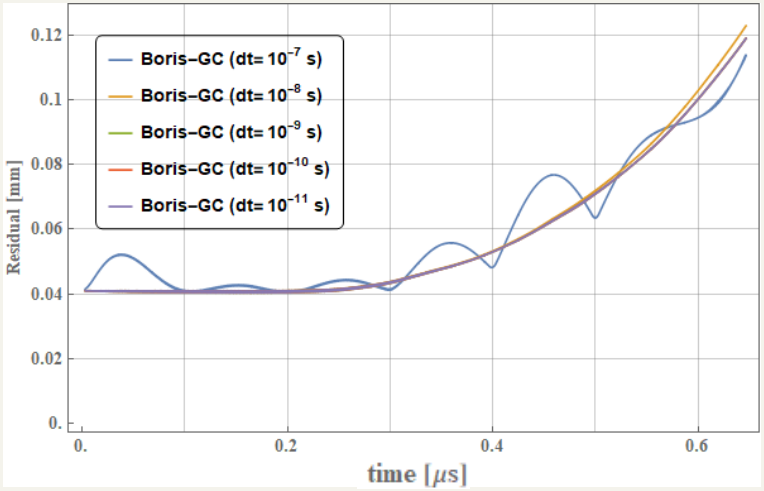

Figure: Boris-GC orbit residual at corresponding propagation times.

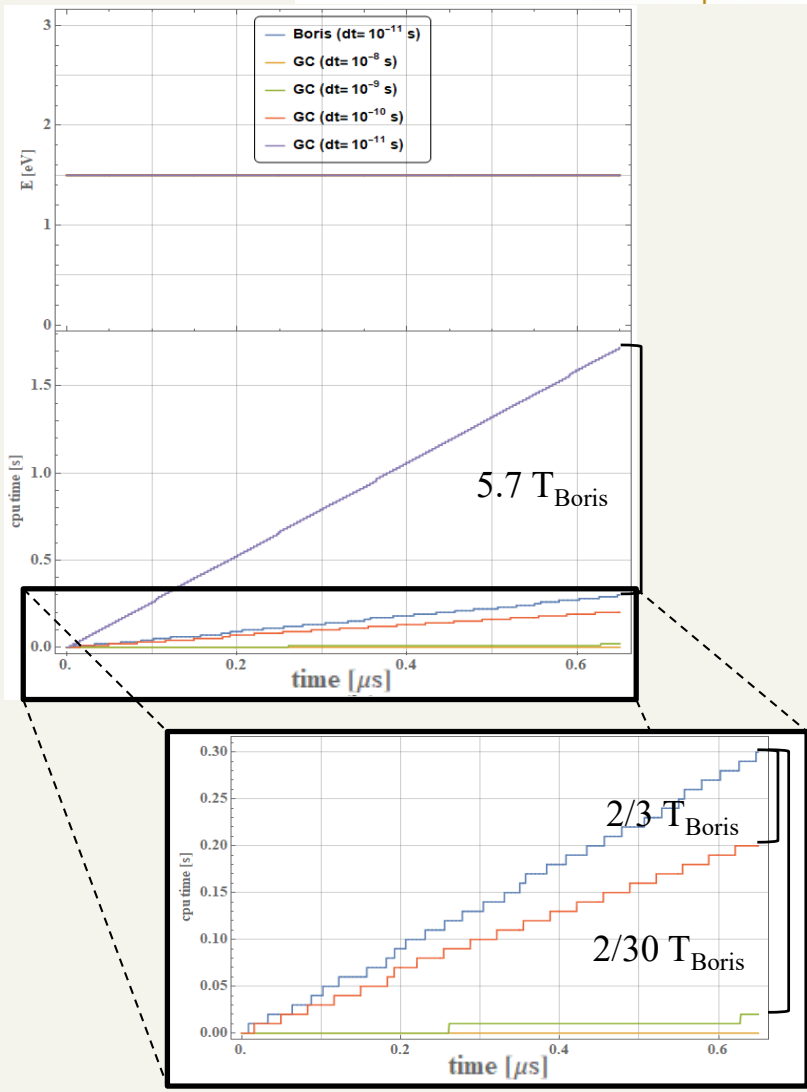

Disphasement FFA

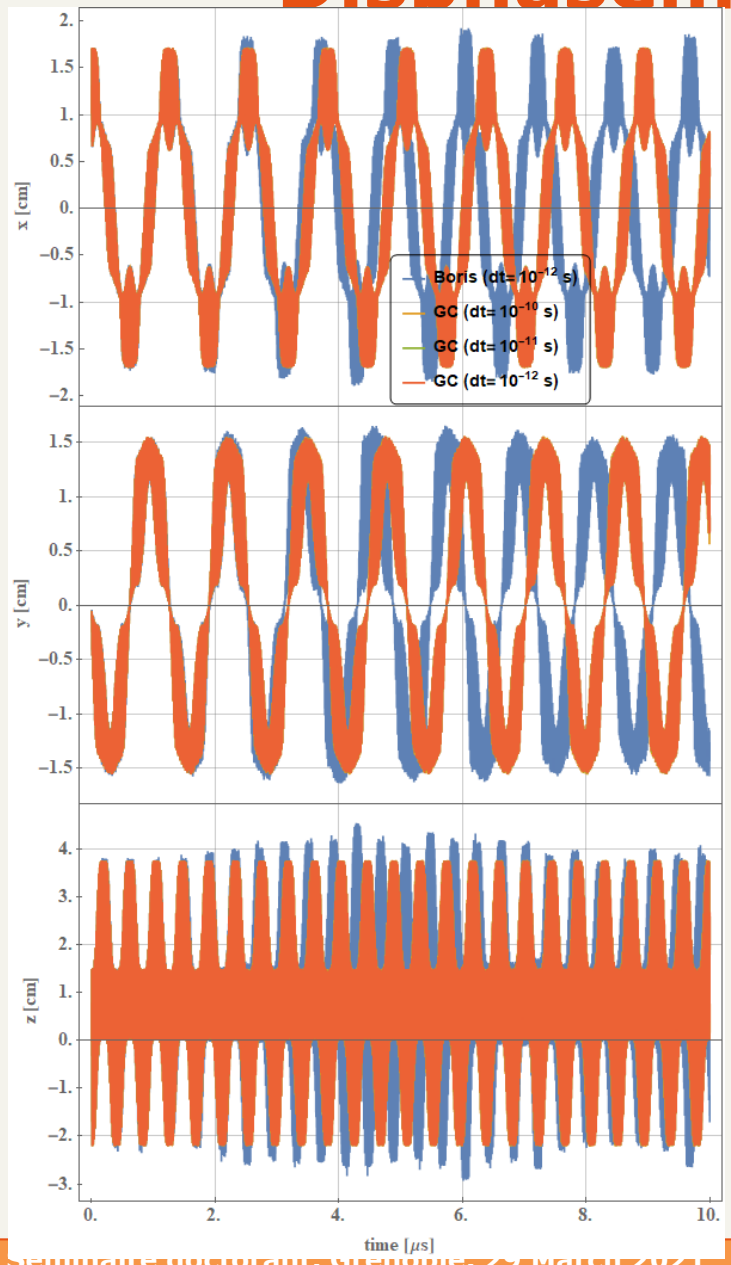

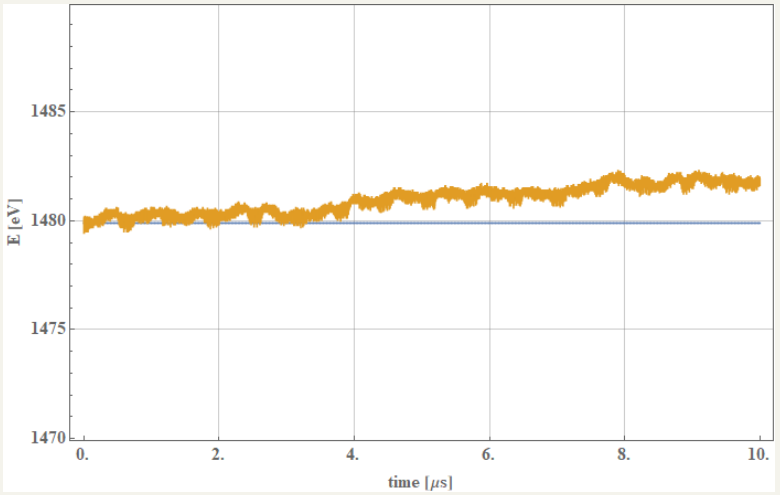

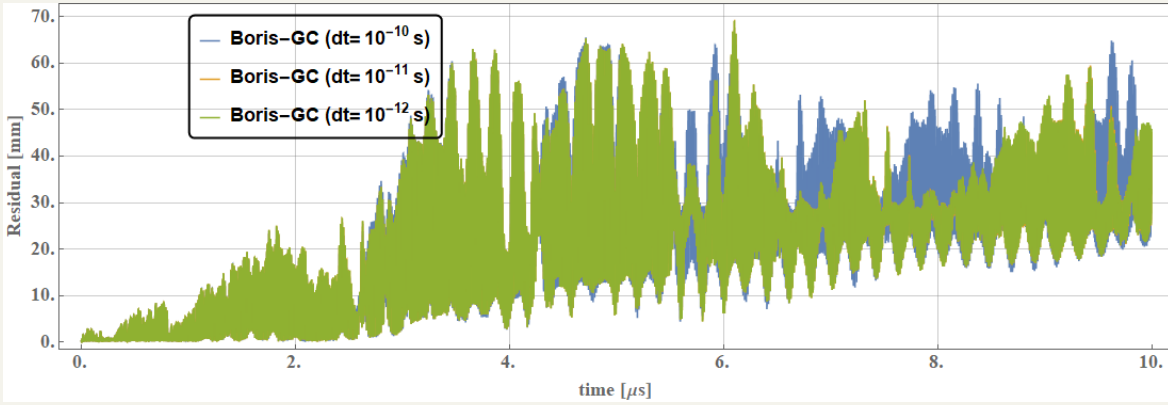

GC approximation validity by electron's kinetic energy

T [eV]	γ	v [m/s]	~$v_\perp$ [m/s]	B [T]	∇B [T/m]	ρ [μm]	B/∇B	(B/∇B)/ρ
1	1.000002	593097	342425	0.64	27	3	0.024	7792
10	1.000020	1875511	1082827	0.64	27	10	0.024	2464
100	1.000196	5930105	3423748	0.64	27	30	0.024	779
1,000	1.001957	18727914	10812566	0.64	27	96	0.024	246
10,000	1.019570	58455268	33749165	0.64	27	306	0.024	78
100,000	1.195695	164352596	94889016	0.64	27	1008	0.024	24
1,000,000	2.956955	282128500	162886965	0.64	27	4279	0.024	6

Table: ECRIS near ECR region

T [eV]	γ	v [m/s]	~$v_\perp$ [m/s]	B [T]	∇B [T/m]	ρ [μm]	B/∇B	(B/∇B)/ρ
1	1.000002	593097	342425	0.102	0.3	19	0.340	17813
10	1.000020	1875511	1082827	0.102	0.3	60	0.340	5633
100	1.000196	5930105	3423748	0.102	0.3	191	0.340	1781
1,000	1.001957	18727914	10812566	0.102	0.3	604	0.340	563
10,000	1.019570	58455268	33749165	0.102	0.3	1918	0.340	177
100,000	1.195695	164352596	94889016	0.102	0.3	6324	0.340	54
1,000,000	2.956955	282128500	162886965	0.102	0.3	26848	0.340	13

Table: MDIS near plasma chamber centre

GC particle pusher Algorithm validity

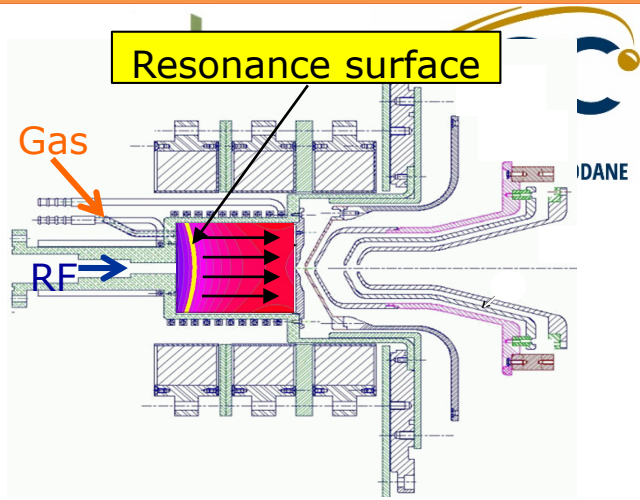

A Magnetic Discharge Ion Source (MDIS) model was used to compare the algorithm's validity in a different regime with a smaller ∇B and shorter electron confinement time

$$\rho_L \ll \frac{B}{|\nabla B|} \quad \Rightarrow \quad \frac{(B/|\nabla B|)}{\rho_L} \gg 1$$

ECRIS (Phoenix V2)

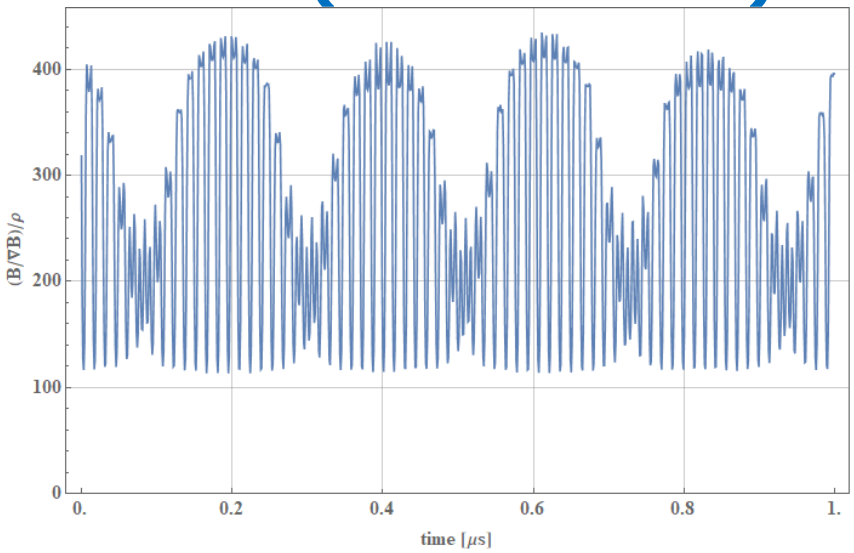

MDIS (SILHI)

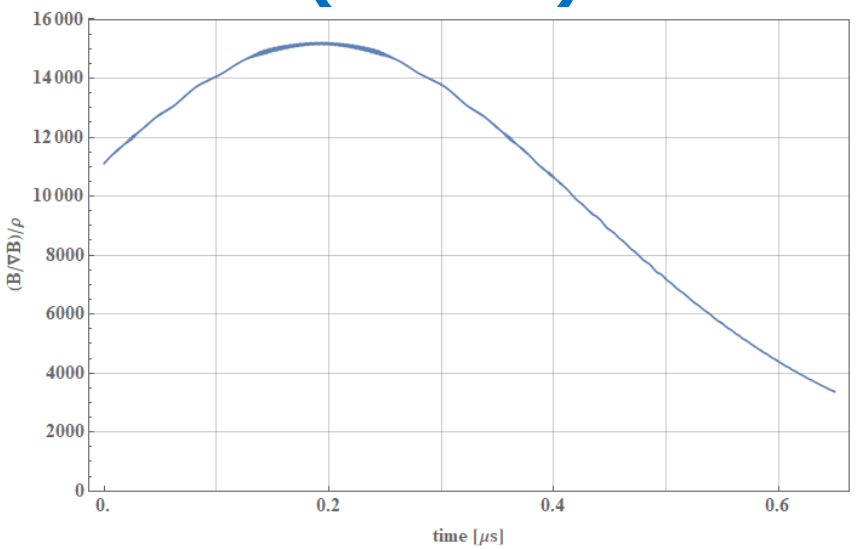

Validity condition for the GC algorithm for ECRIS and MDIS typical orbit

The GC algorithm is more suitable for a MDIS (SILHI type) source than for an ECRIS

GC particle pusher
Conclusions and prospects

- The GC algorithm can accurately reproduce electron trajectories in the following regimes:
  - PHOENIX V2 ECRIS: B=1T, T_e~1keV, volume=0.6L
  - SILHI@GANIL: B=0.1T, T_e~1eV, volume=0.6L
- The GC algorithm can provide an advantage in terms of computation time for particle plasma simulations.
  - For the Phoenix V2 ECRIS the gains are modest, with a time-step increased by a factor of 10^2 and one order of magnitude gain in computation time.
- A smart switcher for orbit integration could be implemented, where the GC approximation is used with a large time-step when valid and a high time orbit resolution isn't required.

-MC ECR plasma simulation- Meshing

- The plasma volume has a $2\pi/3$ rotational symmetry. The plasma chamber mesh can be then defined in that region to save on memory requirements.
- While simulated particles propagate in the whole plasma chamber, their coordinates are assigned to a position on the $2\pi/3$ mesh through rotation.
- A skew mesh is used to better fit the internal edges of the region.

Erosion of the plasma electrode shows plasma symmetry

- Transformation:
  - $y' = y$
  - $x' = cos\left(\theta - \frac{\pi}{2}\right)x + sin\left(\theta - \frac{\pi}{2}\right)y$
    $= sin(\theta)\,x\; - cos(\theta)\,y$
- Inverse:
  - $y = y'$
  - $x = sec(\theta)\,x'\; - cot(\theta)\,y'$

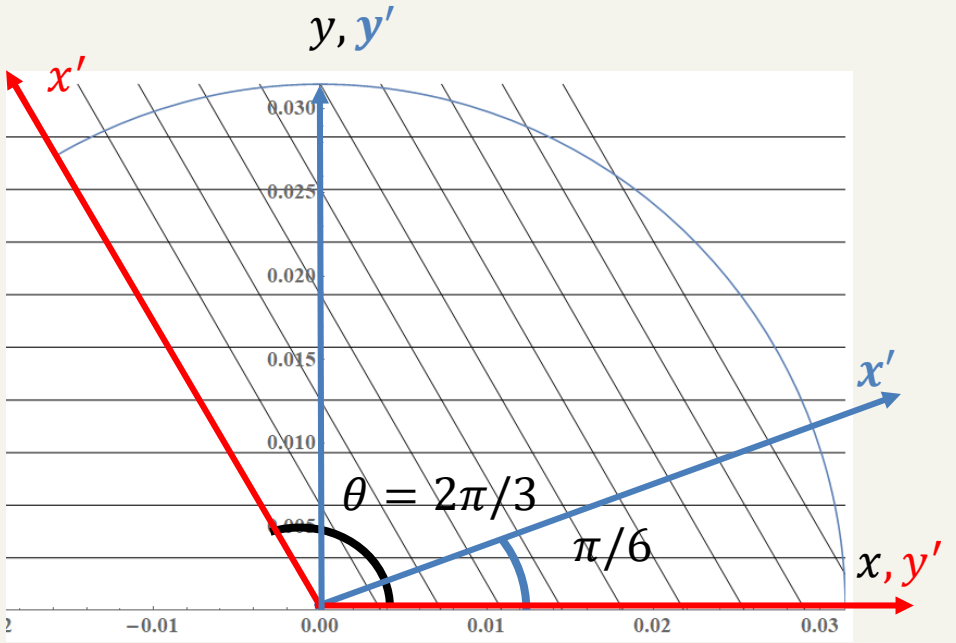

MC ECR plasma simulation Takizuka-Abe method

- Binary collision model
- Requires a pair of particles at each collision step (usually by grouping particles in pairs)
- As we propagate particles independently, we cannot consider pairs so the collision partner is generated from randomly from the distributions at the time.

The scattering angle in TA's method is defined in the relative velocity frame. First two particles with velocity v_α and v_β are selected. Let Θ be the scattering angle between two particles in the relative frame. The angle Θ is sampled randomly through a random variable δ related to Θ by the function tan. Specifically,

$$\delta \equiv \tan(\Theta/2) \tag{2}$$

where δ is a Gaussian random variable which has mean 0 and the following variance

$$\langle \delta^2 \rangle = \left(\frac{e_\alpha^2 e_\beta^2 n_L \log \Lambda}{8\pi\epsilon_0^2 m_{\alpha\beta}^2 u^3} \right) \Delta t$$

where e_α and e_β are electric charges for the species α and β, n_L is the smaller density of the particle species α and β, Λ is the Coulomb logarithm, $u = |v_\alpha - v_\beta|$ is the relative speed, Δt is the time step, and $m_{\alpha\beta}$ is the reduced mass and is defined as follows:

$$m_{\alpha\beta} = \frac{m_\alpha m_\beta}{m_\alpha + m_\beta}.$$

Source: Wang et al. Journal of Computational Physics, Volume 227, Issue 9, (2008)

MC ECR plasma simulation
Sample trajectory - Coulomb

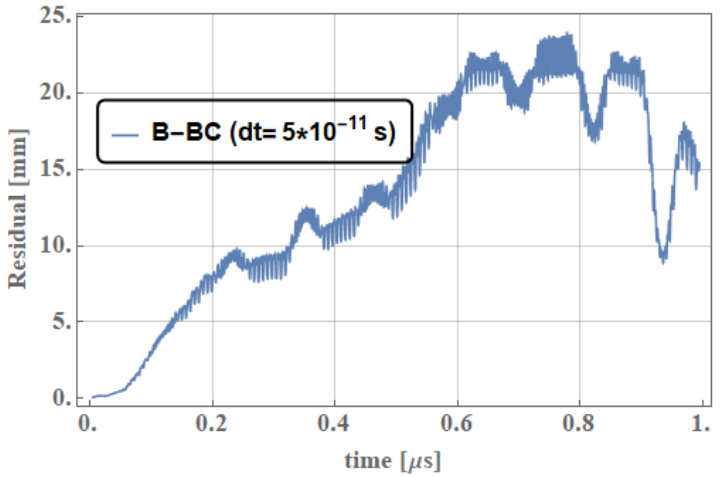

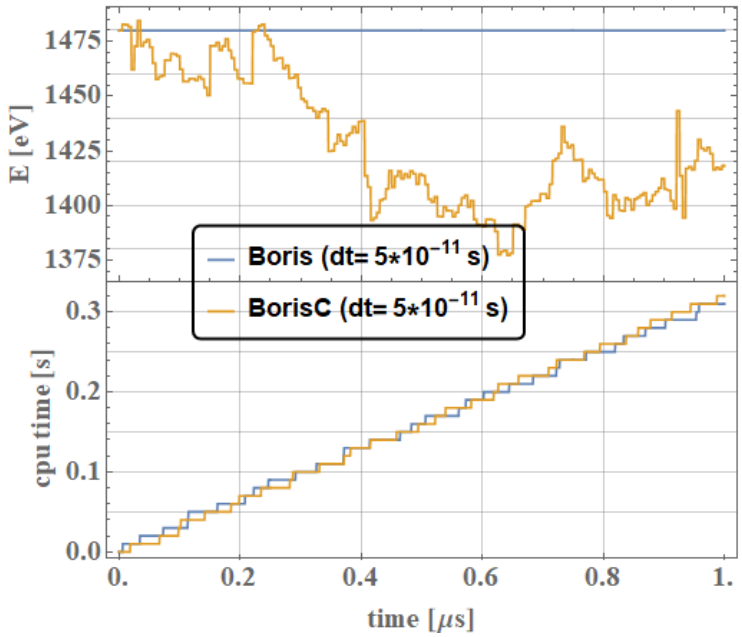

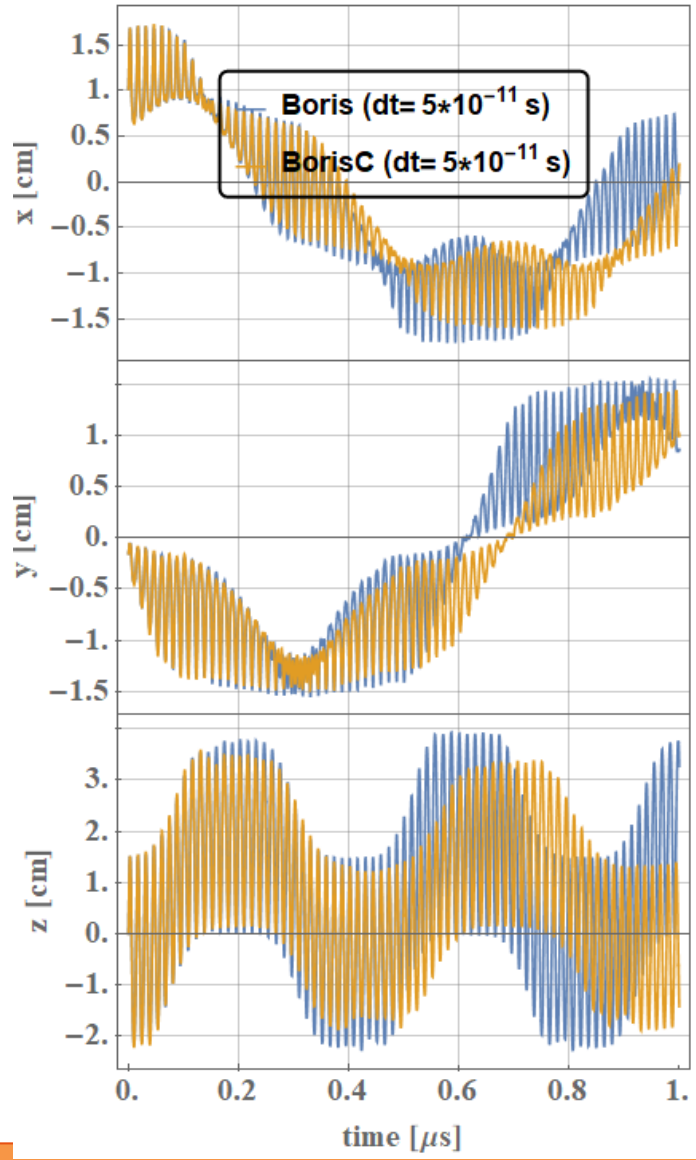

MC ECR plasma simulation
Sample trajectory 2 - Coulomb

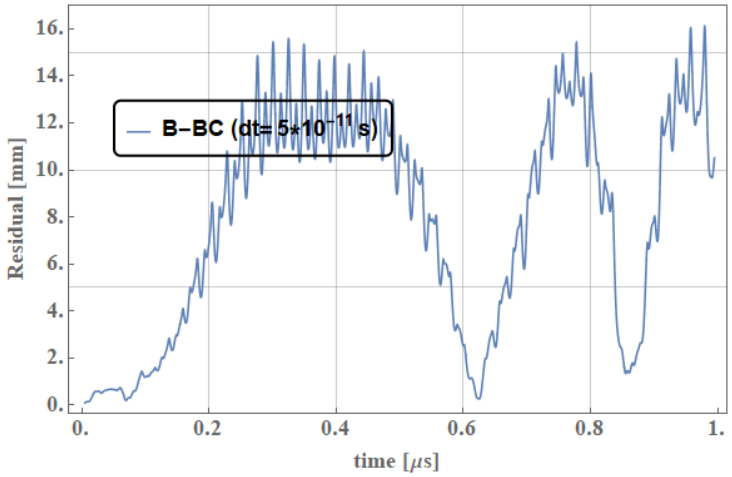

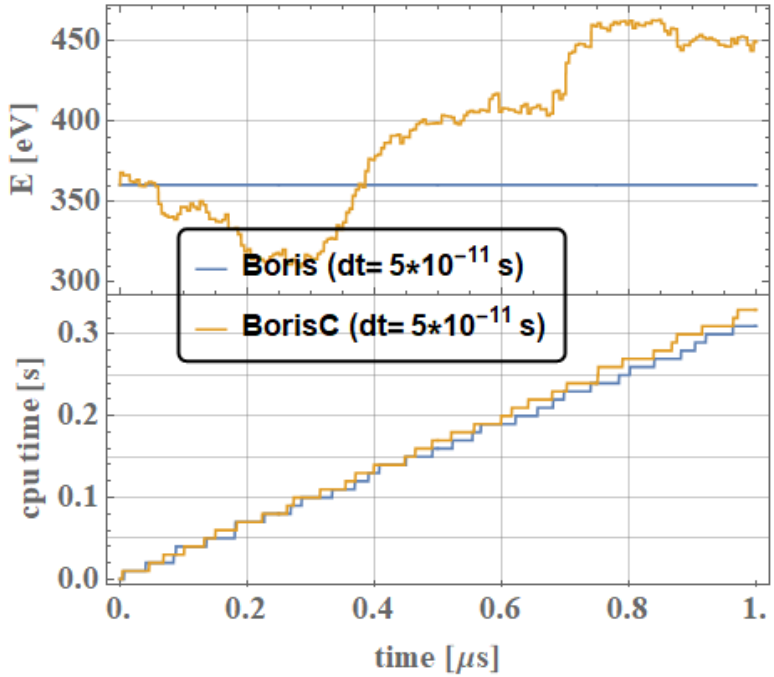

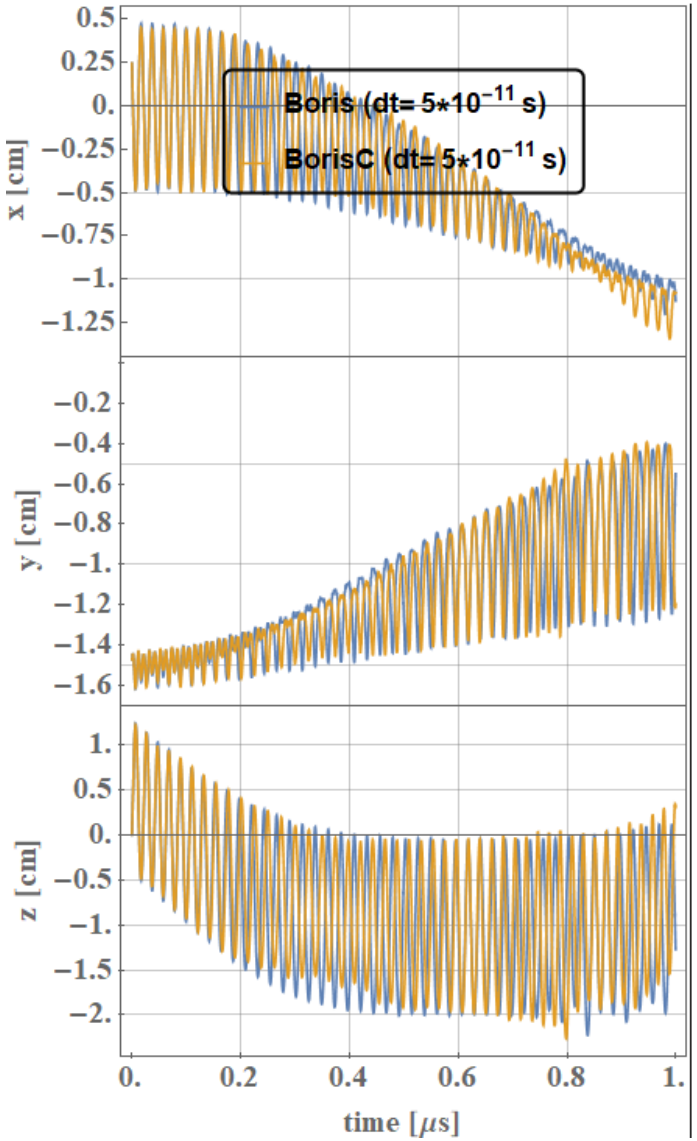

MC ECR plasma simulation
Density distributions coulomb

Density along transverse sections of the mesh

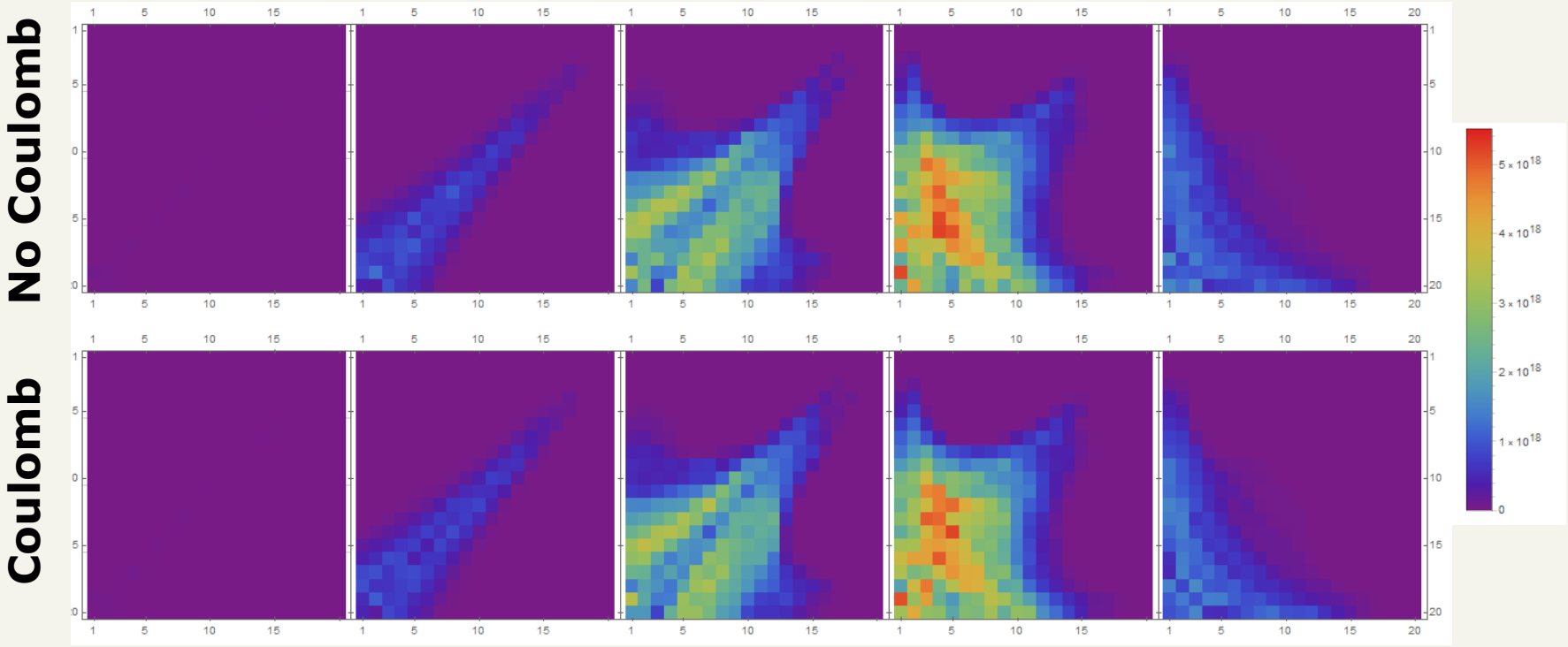

MC ECR plasma simulation
Energy distributions coulomb

Kinetic energy along transverse sections of the mesh

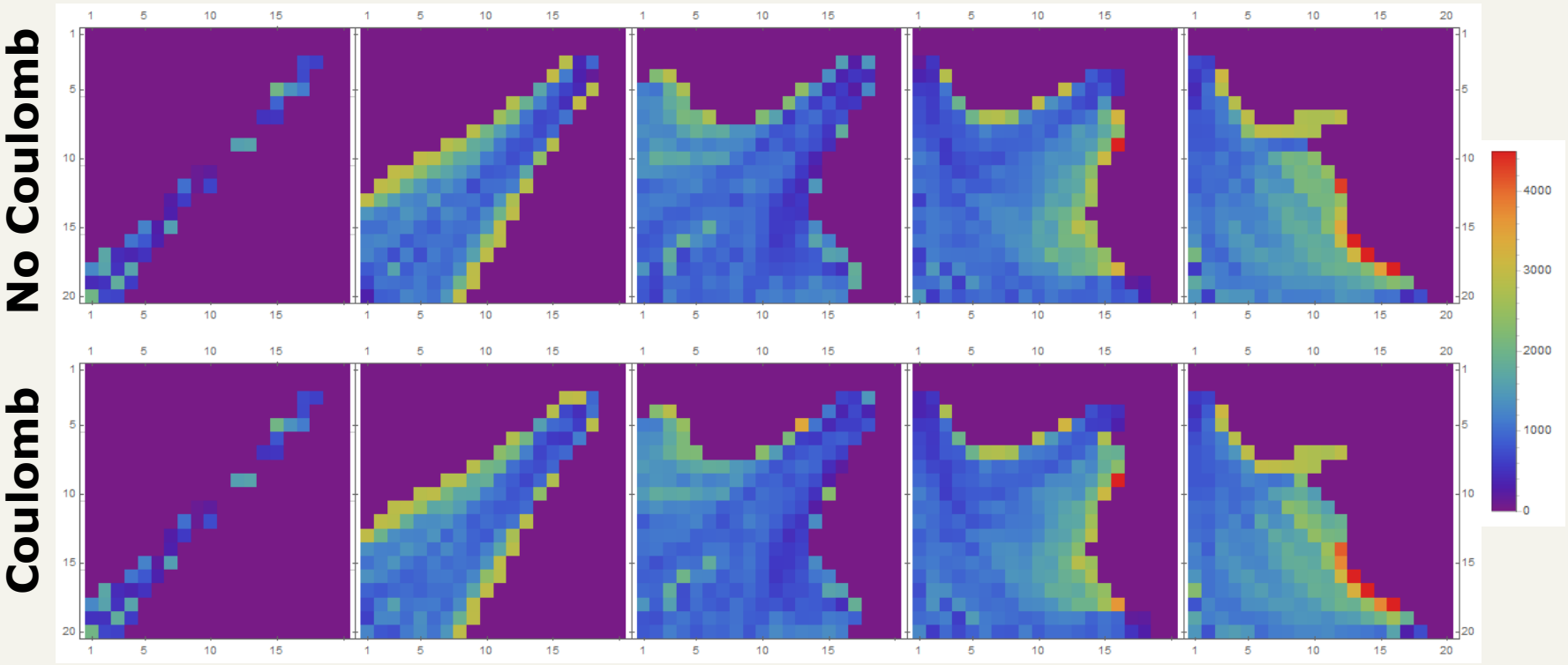

Allison emittance scanner

- In order to validate the model results, experimental measurements of Phoenix V2 beam must be performed.
- Emittance measurement using an Allison scanner will be performed for the 4D transversal emittance.
- This type of scanners use an electric sweep to probe the particle angle distribution, while a mechanical sweep of a slit probes the beam position.
- The relationship between a particle's angle and the potential (V) applied to the electrode plates is as follows: $x'_0 = VL_{eff}/(2gU)$, where qU is the ion's energy, L_{eff} is the effective length of the deflection E field and g is the plate separation.
- To measure the 4D emittance with such a setup, the ability to sweep two perpendicular slits is needed.

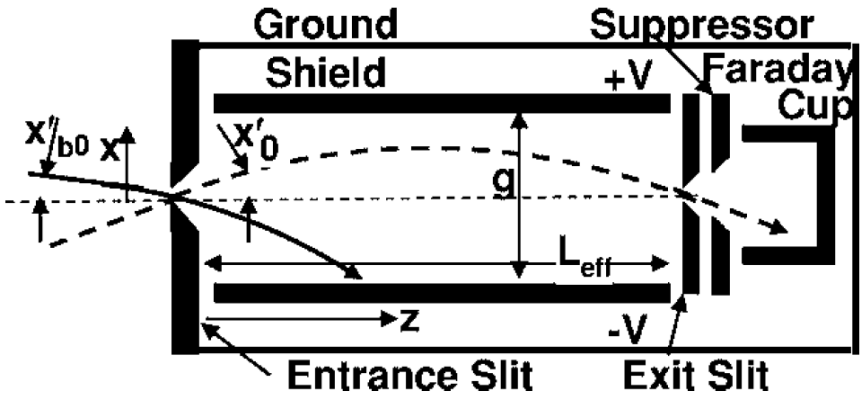

Schema of an Allison scanner (Credit: Stockli, et al.)

State of experiment

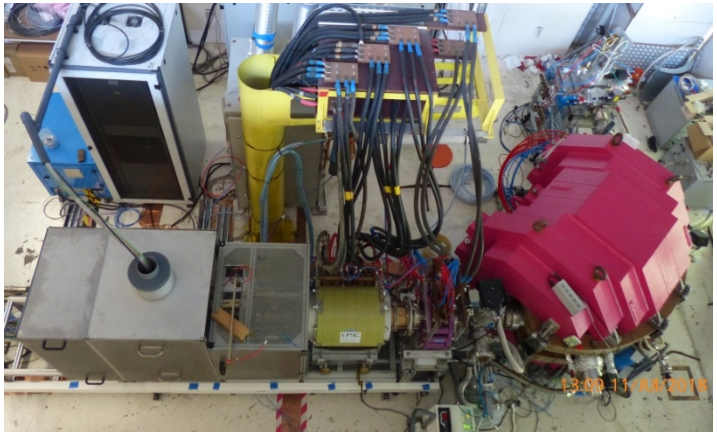

LEBT line at "Banc Fort Courant"

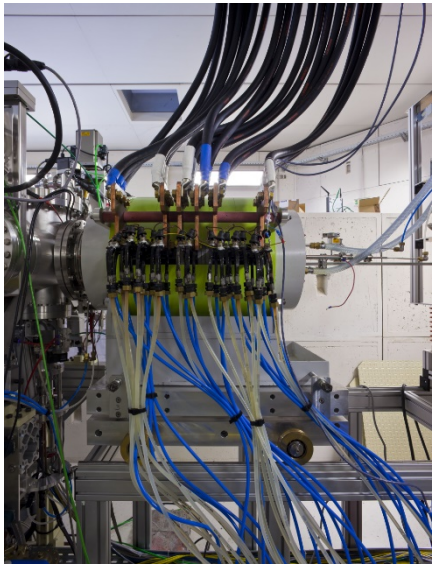

PHOENIX V2 ECR ion source

Movable slit

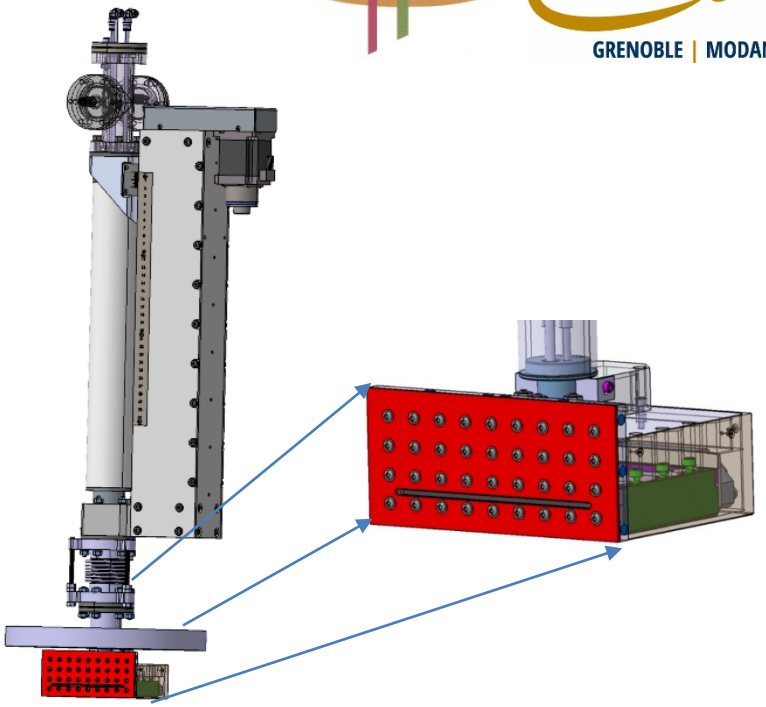

Emittancemeter CAD

- Measure He^{2+} and He^{+} ion beams intensities and emittances vs the ion source free parameters (magnetic field and plasma pressure).
- New detectors to equip on the LEBT
  - Beam dump for beam intensity measurement
  - Allison emittance scanners for the 4D emittance